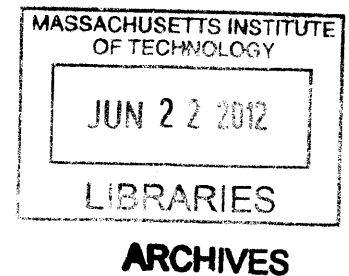


PROCESS FOR OPTIMIZING LOCATION OF DAMPERS IN A BUILDING

By
Vanessa Ampelas

Diplôme d'ingénieur
Ecole Nationale des Ponts et Chaussées, 2012



Submitted to the Department of Civil and Environmental Engineering
In partial fulfillment of the requirements for the Degree of

MASTER OF ENGINEERING IN CIVIL AND ENVIRONMENTAL ENGINEERING
at the
MASSACHUSETTS INSTITUTE OF TECHNOLOGY

June 2012

© 2012 Vanessa Ampelas. All rights reserved

The author hereby grants to MIT permission to reproduce and distribute publicly paper and electronic copies of this thesis document in whole or in part in any medium now known or hereafter created.

Signature of Author: _____
Vanessa Ampelas
Department of Civil and Environmental Engineering
May 11th, 2012

Certified by: _____
Jerome J. Connor
Professor of Civil and Environmental Engineering
Thesis Supervisor

Accepted by: _____
Heidi M. Neft
Chair, Departmental Committee for Graduate Students

PROCESS FOR OPTIMIZING LOCATION OF DAMPERS IN A BUILDING

By
Vanessa Ampelas

Submitted to the Department of Civil and Environmental Engineering on May 11, 2012
in partial fulfillment of the requirements for the Degree of

MASTER OF ENGINEERING IN CIVIL AND ENVIRONMENTAL ENGINEERING
at the
MASSACHUSETTS INSTITUTE OF TECHNOLOGY

ABSTRACT

This thesis is addressing the problem of optimizing the positioning of dampers in a building in order to reduce the cost and achieve a targeted damping for each mode. In order to do so, the thesis is divided into two parts. The first part consists in the study of four traditional configurations of dampers: the diagonal system, the Chevron system, the toggle system and the scissor-jack toggle system. For each configuration the elongation of the damper is calculated without any approximations and the results are used in order to optimize the design of the configuration if it applies, observe its response to horizontal and vertical loading, and extract a linear relationship between the elongation and the perturbation if possible. The second part of the thesis is defining the optimization problem and applying it to a 2D-structure as an example.

Thesis Supervisor: Jerome J. Connor

Title: Professor of Civil and Environmental Engineering

ACKNOWLEDGEMENTS

I would like to express my gratitude to my supervisor, **Professor J. Connor**, who has been of great advice all year-long, for being patient and helping us finding our way while always encouraging us to achieve what we wanted to do.

I would also like to thank **Professor Eric Adams**, Director of the M. Eng Program, for making this great program what it is, and for his availability and kindness.

A very special thanks goes out to our Teaching Assistant, **Pierre Ghisbain**, who has always been available throughout the year, always been patient, and whose help was very appreciable to achieve this thesis.

I would like to acknowledge also **Professor Wierzbicki**, for his support and kindness.

I would also like to thank my friends, my family and all the M.Eng class of 2012, for their help and for all the great time we spent together this year.

TABLE OF CONTENTS

ABSTRACT	2
ACKNOWLEDGEMENTS	3
TABLE OF CONTENTS	4
LIST OF FIGURES	7
INTRODUCTION	10
PART I - STUDY OF TRADITIONAL CONFIGURATIONS OF DAMPERS	11
A. CONFIGURATION 1: THE DIAGONAL SYSTEM.....	12
Sensitivity analysis:.....	12
1. Influence of lateral displacement.....	13
2. Influence of vertical displacement	13
3. Lateral versus vertical displacement.....	14
B. CONFIGURATION 2: THE CHEVRON SYSTEM.....	15
Sensitivity analysis:.....	16
1. Influence of the coordinate x_e	16
2. Influence of the coordinate y_e	18
3. Influence of lateral displacement.....	19
4. Influence of vertical displacement	20
5. Lateral versus vertical displacement.....	21
C. CONFIGURATION 3: THE TOGGLE SYSTEM.....	22
Sensitivity analysis:.....	23
1. Influence of the position of E	23
2. Influence of lateral displacement.....	27
3. Influence of vertical displacement	29
4. Lateral versus vertical displacement.....	30

D.	CONFIGURATION 4: THE SCISSOR-JACK TOGGLE SYSTEM.....	31
	Sensitivity analysis.....	31
	1. Optimum position of E when a given F	31
	2. Optimal position of E and F when symmetrical	35
	3. Influence of lateral displacement.....	35
	4. Influence of vertical displacement	37
	5. Horizontal versus vertical displacement	38
E.	CONCLUSION OF PART I.....	39
	PART II - OPTIMIZATION PROBLEM	40
F.	Mathematical description of the optimization process	40
	1. Definition of the algebraic parameters	41
	2. Definition of the problem.....	44
G.	2D- Example: linking location of dampers and damping ratios achieved	45
	1. Damping ratio target for mode 1 only.....	48
	2. Damping ratio targets for modes 1 and 2	49
	3. Damping ratio targets for modes 1, 2 and 3	51
	4. Damping ratio targets for modes 1, 2, 3 and 4	52
	5. Damping ratio targets for modes 1, 2, 3, 4 and 5.....	53
	6. Damping ratio targets for modes 1, 2, 3, 4, 5 and 6.....	53
	7. Damping ratio targets for mode 12.....	54
	8. Conclusion	55
H.	2D- Example: non-uniform prices.....	55
	1. Damping ratio targeted only for mode 1	56
	2. Damping ratio targeted only for mode 2	58
	3. Damping ratio targeted for modes 1 and 2.....	59
	4. Conclusion	60

CONCLUSION 61

APPENDIXES..... 63

- I- Appendix 1: details of the calculations of the elongation of dampers in configuration 2..... 63
- II- Appendix 2: exact expression of the elongation of dampers in configuration 2 65
- III- Appendix 3: details of the calculations of the elongation of dampers in configuration 67
- IV- Appendix 4: details of the calculations of the elongation of dampers in configuration 4..... 68
- V- Appendix 5: Results of the study of the 2D-structure..... 70

LIST OF FIGURES

Figures 1 and 2: Influence of the lateral displacement when B and C are displaced from 0 to 5% of the total height of the frame (5% of 12=0.60). Left: frame of 12x20, right: frame of 12x30.....	13
Figures 3 and 4: Influence of the vertical displacement when B and C are displaced from 0 to 5% of the total height of the frame (5% of 12=0.60). Left: frame of 12x20, right: frame of 12x30.....	13
Elongations for lateral and vertical displacements for both frames. The relative differences for a same type of load but different frames or same frame but different types of loads are given on the sides.....	14
Figures 5 and 6: Influence of x_e on the elongation of damper 1. Left: frame of 20ftx12ft; right: frame of 30ftx12ft.	17
Figures 7 and 8: Influence of x_e on the elongation of damper 2. Left: frame of 20ftx12ft; right: frame of 30ftx12ft.	17
Figures 9 and 10: Influence of x_e on the total elongation of the dampers: $e_{total} = \sqrt{e_1^2 + e_2^2}$	17
Left: frame of 20ftx12ft; Right: frame of 30ftx12ft.	17
Figures 11 and 12: Influence of y_e on the elongation of damper 1.	18
Left: frame of 20ftx12ft; right: frame of 30ftx12ft.	18
Figures 13 and 14: Influence of y_e on the elongation of damper 1.	18
Left: frame of 20ftx12ft; right: frame of 30ftx12ft.	18
Figures 15, 16 and 17: Total elongation of the dampers for $0 \leq y_e \leq 12$. Zoom for $10 \leq y_e \leq 12$	19
Figures 18, 19 and 20: Frame of 12x20. Influence of the lateral displacement when B and C are displaced from 0 to 5% of the total height of the frame (5% of 12=0.60). From left to right: elongation of the damper n°1, the damper n°2, and the total elongation	20
Figures 21, 22 and 23: Frame of 12x20. Influence of vertical displacement for B and C displaced from 0 to 5% of the total height of the frame (5% of 12=0.60). From left to right: elongation of the damper n°1, n°2 and total elongation	21
Elongations for lateral and vertical displacements for both frames. The relative differences for a same type of load but different positions of E or same position of E but different types of loads are given on the sides.	21
Figures 24 to 26: Plots of the elongation of the damper as a function of x_e and y_e . From left to right: frame of 12x20; frame of 12x30 with no constraint and with the constraint $x_e \in [15,30]$	23
Figures 27: same plot as figure 24 but projected along the z-axis. Figure 28: same as figure 27 but for a displacement ten times smaller ($u_b = u_c = 0.05$). The lines on the surfaces represent equal elevations.	24
Figures 29 and 30: elongation as a function of x_e for $y_e = 2$. The optimum is found for $x_e \approx 7.45$	24
Figures 31 and 32: elongation as a function of x_e for $y_e = 4$. The optimum is found for $x_e \approx 11.05$	25
Figures 33 and 34: elongation as a function of x_e for $y_e = 7$. The optimum is found for $x_e \approx 15.6$	25

Figures 35 and 36: elongation as a function of x_e for $y_e = 9$. The optimum is found for $x_e \approx 18.05$ 25

Figure 37: Representation of the frame 12x30 and the results of the four examples for which y_e was given and $x_{e|opti}$ was found graphically..... 26

Figure 38: Same examples as before but for $u_b = u_c = 0.1$ instead of $u_b = u_c = 0.5$. The table gives the coordinates of the different locations of E studied. 26

Figure 39: representation of the 5 different locations of E studied..... 27

Figures 40 to 45: elongation as a function of u_b for different locations of E and calculations of the slope for the approximation of e as a linear function of u_b 28

Figure 46: illustration of toggle-brace damper configuration with an angle of 90° , in the lower (left) and upper (right) systems (Constantinou et al. 2001, cited in « Analytical and Experimental Study of Toggle-Brace-Damper Systems” by J. Hwang, Y. Huang and Y. Huang, in Journal of Structural Engineering, Vol. 131, No. 7, July 2005). 28

Figures 47 to 52: elongation as a function of v_b for different locations of E and calculations of the slope for the approximation of e as a linear function of v_b 29

Figures 53 and 54: Elongation of the damper as a function of both variables x_e, y_e and zoom 32

Figures 55 to 57: Elongation of the damper as a function of both variables x_e, y_e . Zoom for $x_e \in [12.6;13.0]$ and projection with contours along the z-axis..... 32

Figures 58 and 59: Elongation of the damper as a function of both variables x_e, y_e and projection along the z-axis, for $u_b = u_c = 0.5$ 33

Figures 60 to 62: Elongation of the damper as a function of both variables x_e, y_e for $u_b = u_c = 0.1$ 33

From left to right: complete surface, zoom for $x_e \in [2;3]$ and projection along the z-axis 33

Figures 63 to 65: Elongation of the damper depending on the position of E, for $u_b = u_c = 0.1$. Only one half of the graph should be considered, as y_e has been plotted for 0 to 12 instead of $y_e > \frac{y_c}{x_c} x_e$ 35

Figure 66: Representation of the frame with the different locations of E and F studied 35

Figures 67 to 72: elongation as a function of u_b for different locations of E and calculations of the slope for the approximation of e as a linear function of u_b 36

Figures 73 to 78: elongation as a function of v_b for different locations of E and calculations of the slope for the approximation of e as a linear function of v_b 38

Figure 79. Illustration of how dampers of different type can be located in a building. K and J can have large values. 41

Figure 80: The 2D-asymmetrical structure studied and the K=16 possible locations for dampers. W12x40 sections were used for all beams and W10x33 for all columns 45

Figure 81: From left to right and top to bottom: the shape of the first twelve modes of the 2D-structure 47

Figure 82: shape of mode 1 and the 16 possible locations for dampers. For ease of reading, the red numbers represent the most efficient locations and the blue ones the secondary locations. 48

Figures 83 to 85: From left to right, the shape of modes 1, 2 and 6 and the possible locations for dampers 50

Figures 86 to 88 : From left to right, the shape of modes 1, 2 and 3 and the possible locations for dampers 51

Figures 89: the shape of mode 4 52

Figures 90: the shape of mode 5 and the results of the optimization process for $c = 5, \xi_{5|target} = 10\% - 20\%$. 53

Figure 92: Distribution of the prices throughout the structure. Red represents the most expensive locations, followed by orange and yellow being the cheapest ones. 56

Figures 93 and 94: cases 1 and 2. Comparison between the optimization process when P=1(before) and when P varies (after). In blue: the locations that have a damper in both cases; in yellow, those that differ 57

Figures 95: case 3. Same constraint as in case 1 but with a larger c. 58

Figure 96: case 4 59

Figures 97 and 98: cases 5 and 6 60

INTRODUCTION

This thesis is part of a more general project, the aim of which is to develop a method to quickly obtain a reasonably good evaluation of the seismic response of a building. In current practice, the precise dynamic modeling of buildings takes months to perform and can only be done after the construction has been finished. As the insurance rate can only be defined once these analyses have been carried out, the owner cannot precisely predict the overall cost of his building before constructing it. It is not uncommon to see that a building in good structural shape has to be torn apart after an earthquake because the cost of repairs of non-structural elements and the cost of inoccupation might be greater than the cost of a new building.

The objective of a team at the Massachusetts Institute of Technology is therefore to create a method for creating a simplified model of buildings which would be much faster to analyze while still producing good results. As the analysis would be run very quickly, changes could even be made during the construction depending on what is observed. Ultimately this will allow the owners and insurance companies to come up with an objective of cost and damages for the building to be constructed, reducing the financial uncertainties and increasing the structural stability of the building.

This thesis aids this general objective by studying the optimization process of the installation of dampers in a building. These devices are commonly used to control the building response to wind and earthquake loads, and are characterized by the damping ratio resulting from the force they produce. Given inputs of the shape of the building's dynamic modes and the prices of various dampers, one can optimize which type of dampers should be used and where they should be positioned. In order to do so, the first part of this thesis will study four different configurations of dampers that can be placed within a rectangular structural element. We will look at the exact expression of the elongation of each damper as a function of how the nodes of the frames are displaced. The second part of this thesis focuses on an optimization method that combines these geometrical relationships with knowledge of the dynamic modes of a particular structure and the dollar cost of each element to obtain the best structural configuration. In this case, the best structural configuration is a function of minimum cost and maximum damping of the dynamic modes. A 2-dimensional model is examined in-depth as an example application of this process.

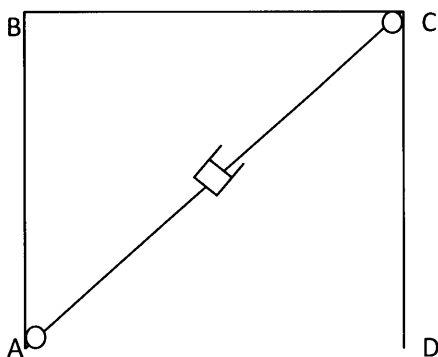
As the first part of this thesis is based on very long symbolic calculations, Maple version 15 has been chosen as the main software; SAP and Excel are used as complements in the second part.

PART I - STUDY OF TRADITIONAL CONFIGURATIONS OF DAMPERS

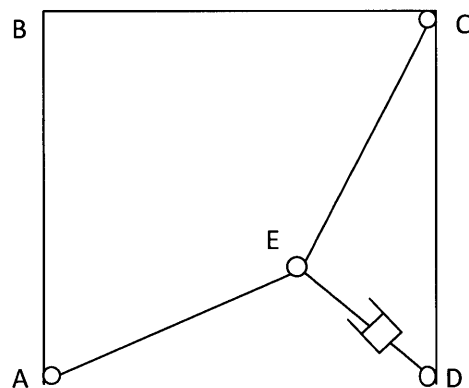
The first part of this thesis is dedicated to the study of four common configurations of dampers: the diagonal system, the Chevron system, the toggle system and the scissor-jack toggle system. For each of them the exact elongation of the dampers depending on the displacements of the nodes A, B, C and D will be calculated. We will solve quadratic equations which results have sometimes more than 1,000 terms. Maple was chosen instead of Matlab because the latter could not handle such symbolic calculations.

The results will then be used to design the optimal shape of the damper system (if it applies) and to study its response to different types of loading. When possible, the approximate linear expression of the elongation will be given. As the calculations are very complicated, these comparisons will be carried out numerically, on two common types of frames: 20 ft wide x 12 ft high and 30 ft wide x 12 ft high.

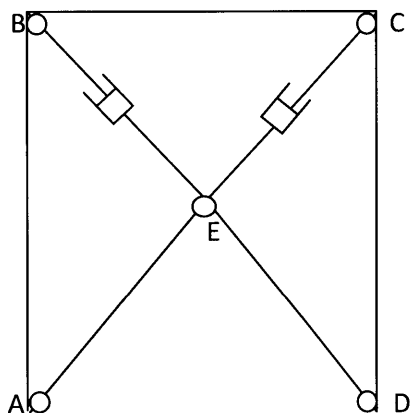
Configuration 1: diagonal system



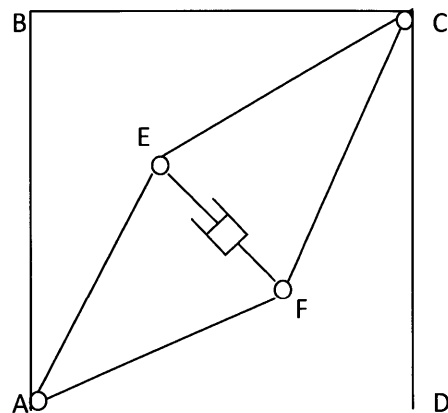
Configuration 3: toggle system



Configuration 2: Chevron system



Configuration 4: scissor-jack toggle system



For all the calculations the same notations for the coordinates of a point will be used, which is to say:

- (x,y) : initial coordinates of the node
- (u,v) : displacements of the node
- $(X=x+u,Y=y+v)$: final coordinates of the node

The assumptions that will be used for this study are:

- The members which carry dampers can elongate.
- The members of the frame that are not carrying dampers are rigid and inextensible; however, the small vertical displacement of a vertical beam displaced horizontally is neglected. This is done to ensure loads are only applied in a single direction.
- The initial and final positions of A, B, C, D are known.
- The initial position of E and F, if applicable, is known.
- The loadings will range from 0 to 5% of the height of the frame. As 5% is a large deformation, in a few cases this range is reduced.

A. CONFIGURATION 1: THE DIAGONAL SYSTEM

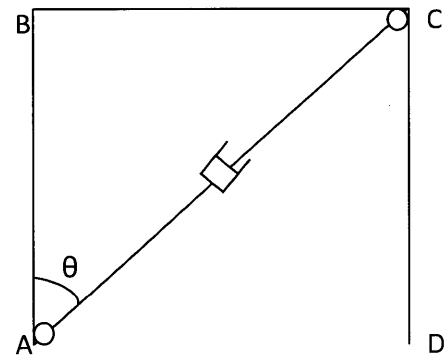
As this configuration is geometrically simple, the calculation of the damper elongation is straightforward.

The elongation is defined as the initial length of the member AC minus its final length.

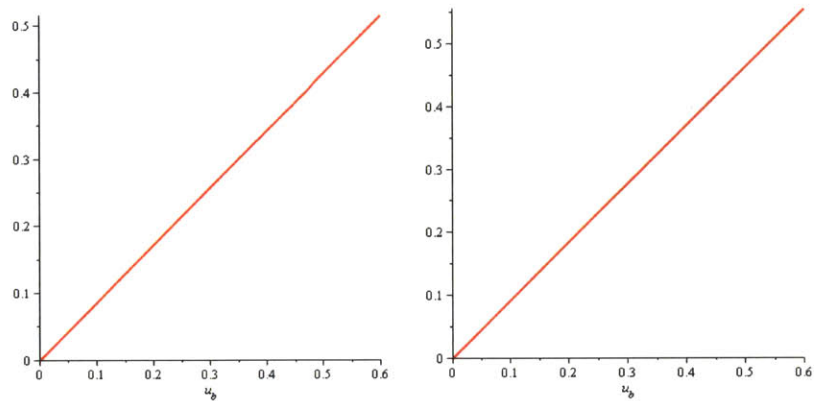
$$e = \sqrt{(x_C + u_C - x_A - u_A)^2 + (y_C + v_C - y_A - v_A)^2} - \sqrt{(x_C - x_A)^2 + (y_C - y_A)^2}$$

Sensitivity analysis:

The numerical examples are carried out by displacing B and C the same amount, either laterally or vertically. Physically these cases correspond to the lowest order dynamic modes; entire stories of the building move in unison at much lower frequencies than those required to generate intra-floor vibrations.



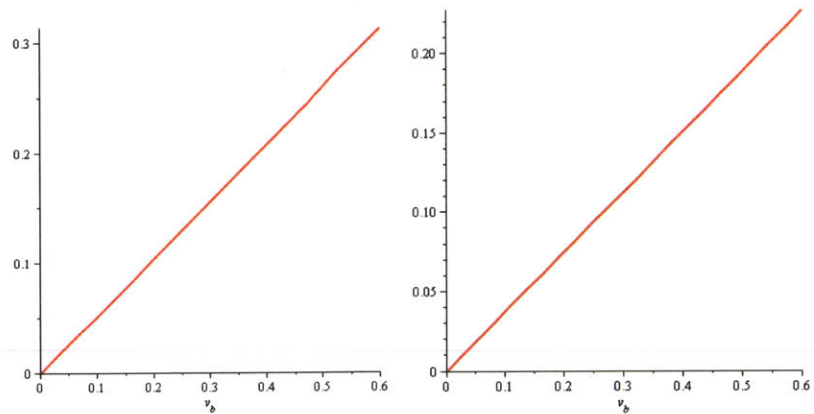
1. Influence of lateral displacement



Figures 1 and 2: Influence of the lateral displacement when B and C are displaced from 0 to 5% of the total height of the frame (5% of 12=0.60). Left: frame of 12x20, right: frame of 12x30.

It can be seen that the displacement is very nearly linear in both cases, but the slope slightly changes from $0.860824 \approx \frac{20}{\sqrt{12^2 + 20^2}}$ to $0.929736 \approx \frac{30}{\sqrt{12^2 + 30^2}}$. The relative difference between these results and the commonly accepted approximation $e \approx u_b \cdot \sin \theta$, are: 0.1356% for the 20ftx12ft frame and 0.3885% for the 30ftx12ft frame. A good approximation of the elongation is therefore $e \approx u_b \cdot \sin \theta$.

2. Influence of vertical displacement



Figures 3 and 4: Influence of the vertical displacement when B and C are displaced from 0 to 5% of the total height of the frame (5% of 12=0.60). Left: frame of 12x20, right: frame of 12x30.

It can be seen that the displacement is very nearly linear in both cases, but the slope changes from $0.523829 \approx \frac{12}{\sqrt{12^2 + 20^2}}$ to $0.379339 \approx \frac{12}{\sqrt{12^2 + 30^2}}$. The relative difference between these results and the commonly accepted approximation $e \approx u_b \cdot \cos \theta$, are: 1.814% for the 20ftx12ft frame and 2.1403% for the 30ftx12ft frame. A good approximation of the elongation is therefore: $e \approx u_b \cdot \cos \theta$.

3. Lateral versus vertical displacement

	Lateral displacement $u_b = u_c = 0.6$	Vertical displacement $v_b = v_c = 0.6$	Relative difference for the same frame
Frame of 12x20	0.516	0.314	64.33%
Frame of 12x30	0.558	0.228	144.74%
Relative difference for a same type of displacement	8.14%	37.72%	

Elongations for lateral and vertical displacements for both frames. The relative differences for a same type of load but different frames or same frame but different types of loads are given on the sides.

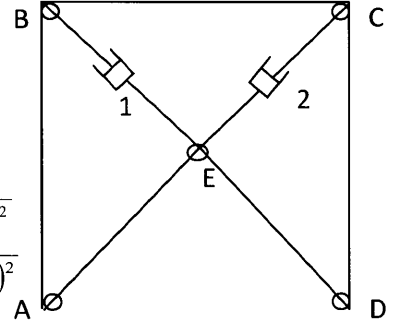
From this table it can be concluded that this configuration is much more efficient for a lateral displacement than for a vertical displacement with these two frame sizes (going up to nearly 150% relative efficiency). Then, by taking a closer look at the influence of the size of the frame, it can be noticed that the wider the frame is the better for a lateral displacement, but the taller the better for a vertical displacement. As a conclusion, this configuration should be used for a lateral displacement within these two frame sizes. The approximate elongation, which can also be derived analytically, is then: $e \approx u_b \cdot \sin \theta$.

B. CONFIGURATION 2: THE CHEVRON SYSTEM

This configuration has two dampers placed symmetrically in a structure that is itself symmetrical. Both elongations are functions of the unknowns u_e and v_e which characterize the displacement of E.

$$e_{damper1} = \sqrt{(x_B + u_B - x_E - u_E)^2 + (y_B + v_B - y_E - v_E)^2} - \sqrt{(x_B - x_E)^2 + (y_B - y_E)^2}$$

$$e_{damper2} = \sqrt{(x_C + u_C - x_E - u_E)^2 + (y_C + v_C - y_E - v_E)^2} - \sqrt{(x_C - x_E)^2 + (y_C - y_E)^2}$$



In order to calculate the displacement of E, both members AE and ED are assumed to be rigid and therefore with constant length. These two equations then lead us to a system of two equations for two unknowns. The only problem is that they are quadratic equations and not linear ones. The resulting system is expressed with a quadratic equation for v_e and a linear expression for u_e depending on v_e . The details of the calculations are given in Appendix 1.

$$\Rightarrow \begin{cases} u_E = -v_E \xi + \varphi \\ v_E^2 (1 + \xi^2) + 2v_E (\beta - \varphi \xi - \alpha \xi) + \varphi^2 + 2\alpha \varphi + u_A \gamma + v_A \delta = 0 \end{cases}$$

The calculation of the discriminant is useful as an intermediate check. If the discriminant is negative, there will be no solution to the problem and the coordinates need to be changed. For most configurations this occurs when the assumed displacements are too large. Effectively, if (u,v) are of the order of 1% of the (x,y) coordinates, then the discriminant is reduced by approximation to a positive

$$\text{number: } \Delta = \left(x_e - x_a - \frac{(y_e - y_a)(x_d - x_a)}{y_d - y_a} \right)^2.$$

Then we finally solve for u_e and v_e . As this study is made in order to get the full expressions, the reasoning is made from a mathematical point of view and not from a physical point of view. Therefore two results are obtained for v_e , which leads to two possible values for u_e . Both expressions of the final elongation are extremely long and are therefore only given in Appendix 2.

The two solutions correspond to the position of E being in the frame and its symmetrical position with regards to (AD). For mathematical correctness those two solutions are kept until the end, but for the numerical examples, the results will be only given for the physical solution.

Sensitivity analysis:

For all numerical examples both types of frames, 20ftx12ft and 30ftx12ft, will be studied.

As two dampers are linked to the same point E, the results of the elongations will first be given for both dampers and then for the total elongation $e_{total} = \sqrt{e_1^2 + e_2^2}$. This “total elongation” does not have a physical meaning as $|e_1| + |e_2|$ does for example, but it corresponds to the contribution of both dampers to the frame. e_{total} will also be used in the second part of this thesis for the normalized contribution of

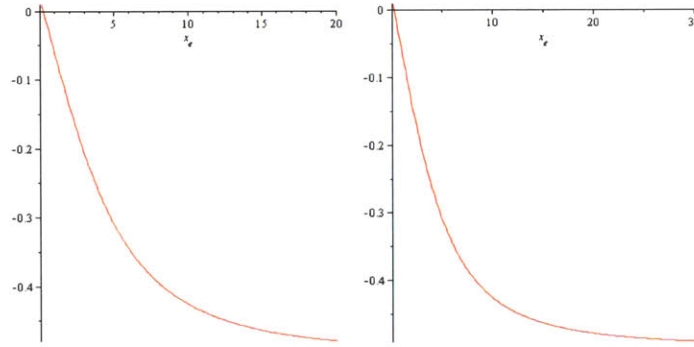
location k to the damping ratio of mode m, which is given by $x_{mk}(j) = \frac{e_{km}^2(j)}{2\sqrt{k_m \mu_m}}$, where

$e_{km} = \sqrt{e_{1m}^2 + e_{2m}^2}$ and e_{1m}, e_{2m} are the elongations of both dampers in mode m shape of mode m.

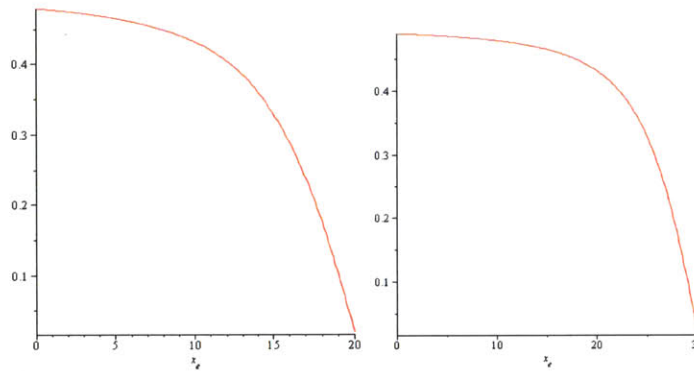
As the initial position of E is extremely important, the influence of the coordinates (x_e, y_e) on the elongation of the dampers will first be studied. Then a vertical or horizontal load ranging from 0 to 5% of the height of the frame will be applied.

1. Influence of the coordinate x_e

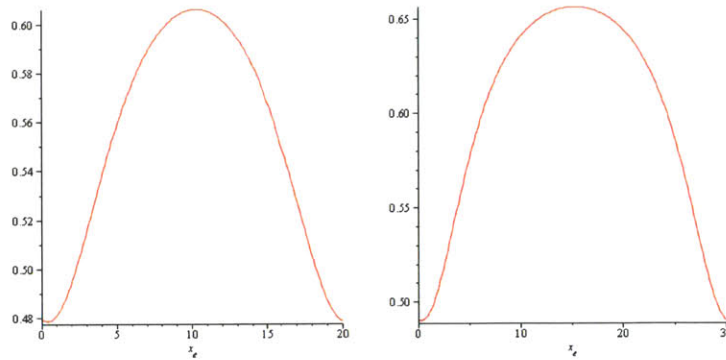
In this first geometry optimization study the coordinate x_e can vary from 0 to 20 (or 30) and we have chosen $y_e = 6$. Since the lateral load is the most common one in seismic design, we applied a lateral displacement of 0.5 to B and C, which corresponds to a lateral displacement of 4.2% of the height. The results of the influence of x_e are given underneath.



Figures 5 and 6: Influence of x_e on the elongation of damper 1. Left: frame of 20ftx12ft; right: frame of 30ftx12ft.



Figures 7 and 8: Influence of x_e on the elongation of damper 2. Left: frame of 20ftx12ft; right: frame of 30ftx12ft.



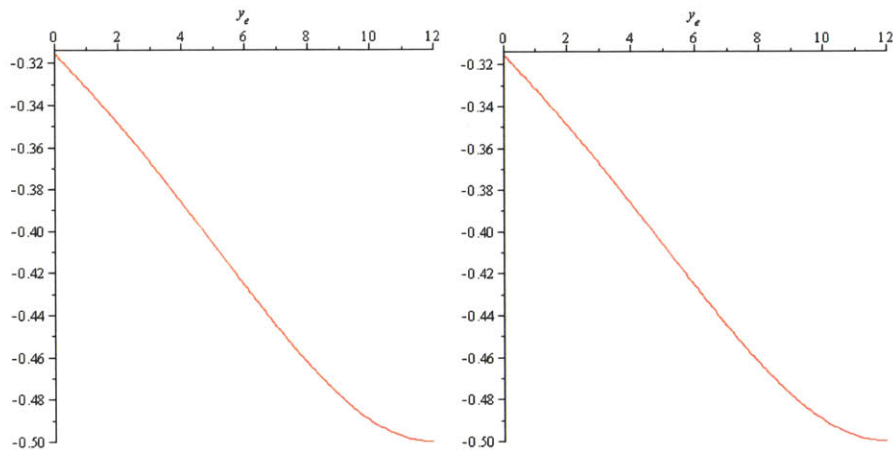
Figures 9 and 10: Influence of x_e on the total elongation of the dampers: $e_{total} = \sqrt{e_1^2 + e_2^2}$

Left: frame of 20ftx12ft; Right: frame of 30ftx12ft.

As a conclusion, it can first be noted that the width of the frame does not influence the general shape of the curves. The results are coherent as the elongation of the damper 1 is maximized if E is on the member CD and vice versa. Since the system is symmetrical there were two possibilities for the maximum total elongation: either when one of the dampers is fixed to a vertical member or when E is placed in the middle. It appears that the maximum total elongation is actually when E is on the perpendicular bisector of the top member BC.

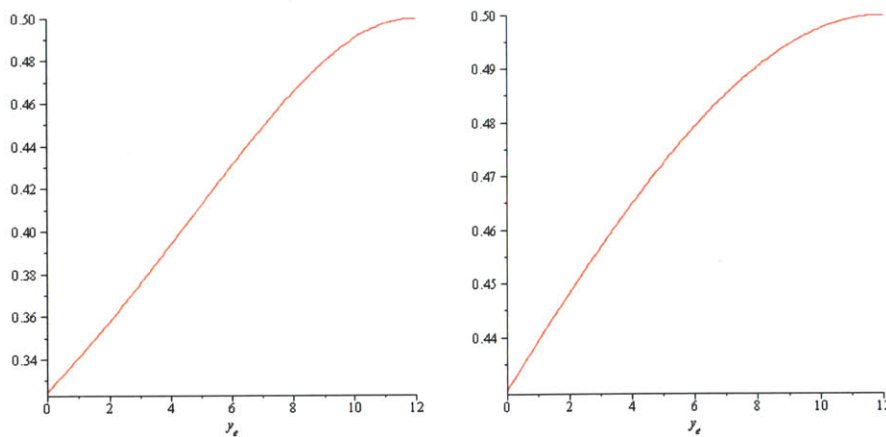
2. Influence of the coordinate y_e

In this second case study the coordinate y_e can vary from 0 to 12 in both frames and $x_e = \frac{x_a + x_d}{2}$. As the lateral load is the most common one in seismic design, a lateral displacement of 0.5 was applied to B and C, which corresponds to a lateral displacement of 4.2% of the height. The results of the influence of y_e are given underneath, the plots on the left being for the frame 20ftx12ft and those on the right for the frame of 30ftx12ft.



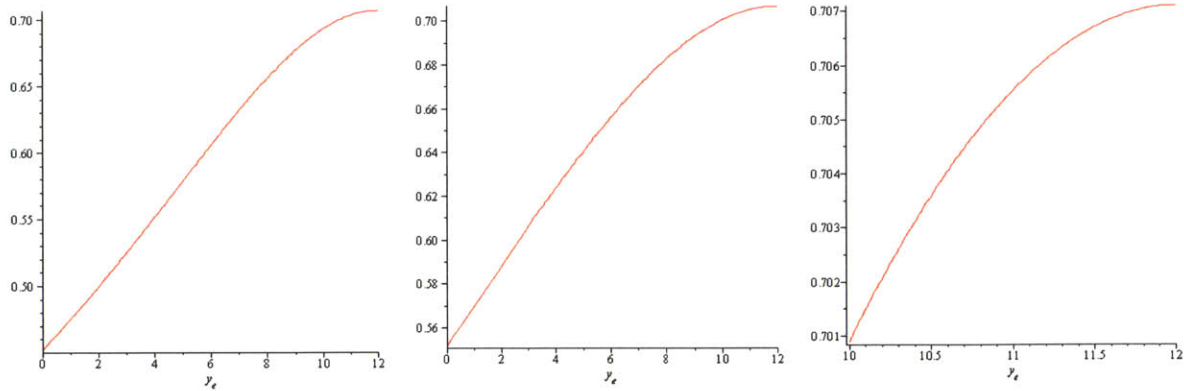
Figures 11 and 12: Influence of y_e on the elongation of damper 1.

Left: frame of 20ftx12ft; right: frame of 30ftx12ft.



Figures 13 and 14: Influence of y_e on the elongation of damper 1.

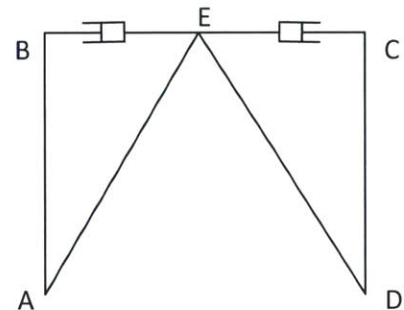
Left: frame of 20ftx12ft; right: frame of 30ftx12ft.



Figures 15, 16 and 17: Total elongation of the dampers for $0 \leq y_e \leq 12$. Zoom for $10 \leq y_e \leq 12$

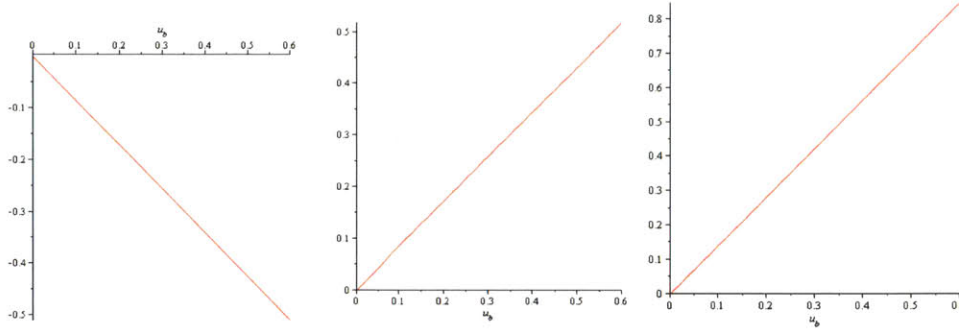
As a conclusion, it can first be noted that the width of the frame does not influence the general shape of the curves, which was expected as the vertical influence of E is studied. It seems that all curves tend to an asymptote when y_e reaches 10. A close-up on the total elongation shows that the maximum is attained for $y_e = 12$, which is to say when E is on the top member of the frame, but if $y_e = 10$ instead of 12, it leads to 98% of the maximum total elongation. This means that if a damper cannot be put exactly into the floor, results can still be good by putting it close to it.

As a conclusion of the first two case studies, the ideal position of E for the configuration 2 is when E is placed on the top element of the frame BC, as shown on the figure.



3. Influence of lateral displacement

The same lateral displacement was applied to B and C in order to see the influence of lateral displacements on the elongation of the dampers. The applied displacement is such that $u_b = u_c$ range from 0 to 5% of the height of the frame (5% of 12 being 0.60). The results are given for the initial position of E being in the middle of the frame: E(10,6).



Figures 18, 19 and 20: Frame of 12x20. Influence of the lateral displacement when B and C are displaced from 0 to 5% of the total height of the frame (5% of 12=0.60). From left to right: elongation of the damper n°1, the damper n°2, and the total elongation

The shapes of the curves are still varying linearly for:

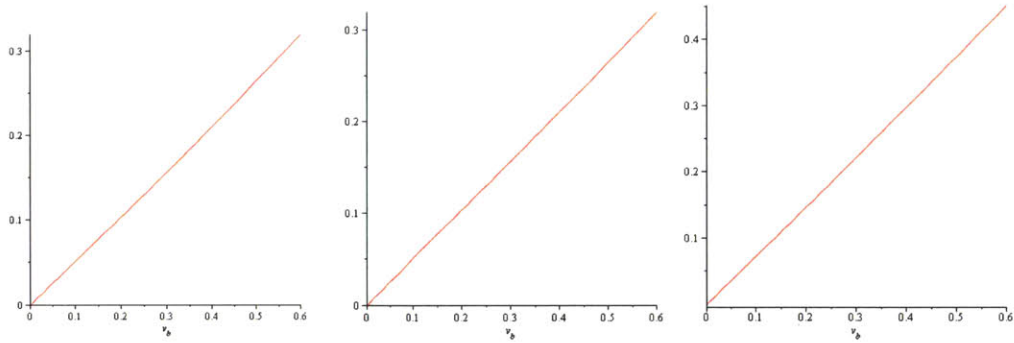
- a frame of 30x12, but the values are slightly higher
- another random initial position of E.

For numerical comparison, for a frame of 12x20, the total elongation when $u_b = u_c = 0.6$ is: 0.832 for E(10,10) and 0.727 for E(10,6). The relative difference is of 14.4%.

The slope of the total elongation when E is originally placed in the optimal position E(10,12) or E(15,12) is such that $e_{total} \approx 1.4 \cdot u_b \approx \sqrt{2} \cdot u_b$. For another definition of the total elongation: $e_{total} = |e_1| + |e_2|$, the result would have been: $e_{total} = 2 \cdot u_b$, which is the result that can actually be seen when drawing this kind of examples.

4. Influence of vertical displacement

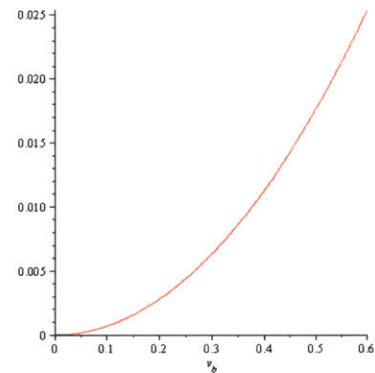
The same vertical displacement was applied to B and C in order to see the influence of lateral displacements on the elongation of the dampers. The applied displacement is such that $v_b = v_c$ range from 0 to 5% of the height of the frame (5% of 12 being 0.60). The results are given for the initial position of E being in the middle: E(10,6).



Figures 21, 22 and 23: Frame of 12x20. Influence of vertical displacement for B and C displaced from 0 to 5% of the total height of the frame (5% of 12=0.60). From left to right: elongation of the damper n°1, n°2 and total elongation

The results are similar to the case study of the influence of lateral displacement but the values are nevertheless quite different, as for E(10,6) we get: $e_{total} = 0.75 \cdot v_b$.

Although the elongations vary linearly for random positions of E, if E is in its optimal position then the curve becomes very different. If a linear fitting is used as an approximation for v_b ranging from 0.4 to 0.6, then: $e_{total} = 0.09987 \cdot v_b$. This change was predictable as if E is positioned on the top frame, a vertical displacement will have little effect.



5. Lateral versus vertical displacement

A table giving the elongations for different locations of E and different types of loading is given for numerical comparison.

	Lateral displacement $u_b = u_c = 0.6$	Vertical displacement $v_b = v_c = 0.6$	Relative difference for the same position of E
E (10,6)	0.727	0.452	60.8%
E (10,10)	0.832	0.190	338%
Relative difference for a same type of displacement	-12.6%	137.9%	

Elongations for lateral and vertical displacements for both frames. The relative differences for a same type of load but different positions of E or same position of E but different types of loads are given on the sides.

Although the absolute difference values seem to be very close, by looking at the relative difference values, it can be seen that the percentages are very high. Also, the relative difference for the same initial position of E, without taking the extreme value of E being on the top member BC, shows that this configuration of dampers is much more efficient for a lateral displacement than for a vertical displacement (up to more than 209%). Lastly, the relative difference for lateral displacement proves that the initial position is also of influence (up to more than 13%).

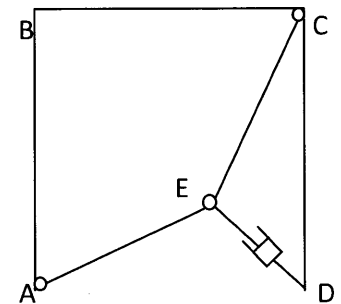
As a conclusion of these case studies, it can be said that the configuration 2 is to be used for lateral displacements, and that the optimal location for point E is to be centered on the horizontal axis and as high as possible on the vertical axis, ideally on the top member BC. For an initial position of E (10,10) and for a lateral displacement of 0.6, the total elongation is 0.832 which means that the amplification is already of 139% when E is positioned only to 83.3% of its optimal height. For a worse initial position of E (10,6), the total elongation is 0.727 which still means that the lateral displacement has been amplified by the dampers by 121% when E is positioned only to 50% of its optimal height.

C. CONFIGURATION 3: THE TOGGLE SYSTEM

The calculation of the elongation of the toggle system proceeds along the same lines as that of the Chevron system. The elongation is first calculated as a function of the coordinates of E and D.

$$e = \sqrt{(x_D + u_D - x_E - u_E)^2 + (y_D + v_D - y_E - v_E)^2} - \sqrt{(x_D - x_E)^2 + (y_D - y_E)^2}$$

The unknowns u_e and v_e are calculated by solving the system expressing the fact that the elements AE and EC are rigid and cannot elongate. The details of the calculations are given in Appendix 3. The elongation can then be calculated.



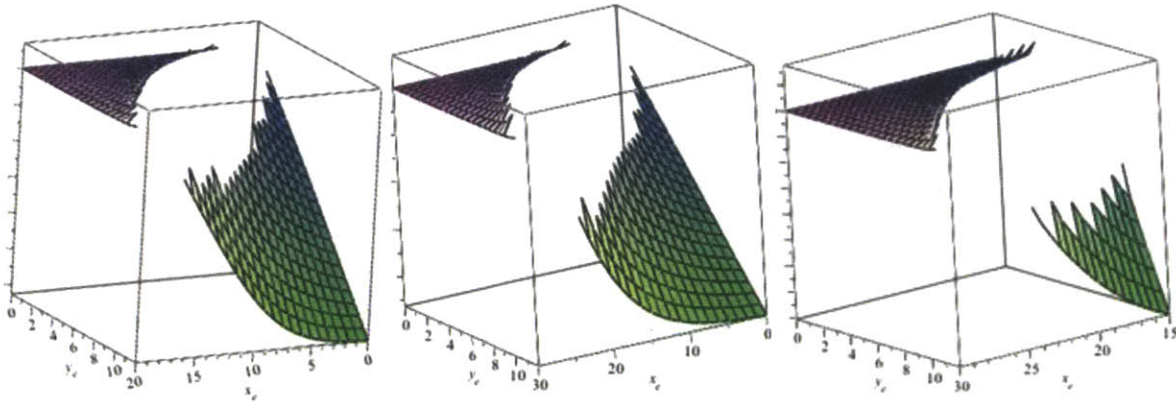
$$\Rightarrow \begin{cases} u_E = -v_E \xi + \varphi \\ v_E^2 (1 + \xi^2) + 2v_E (\beta - \varphi \xi - \alpha \xi) + \varphi^2 + 2\alpha \varphi + u_A \gamma + v_A \delta = 0 \end{cases}$$

Sensitivity analysis:

First of all study the influence of the position of E is studied for a given lateral/vertical displacement of 4% of the height of the frame ($u_b = u_c = 0.5$). Then E is set to its optimal position and the influence of displacements is studied.

1. Influence of the position of E

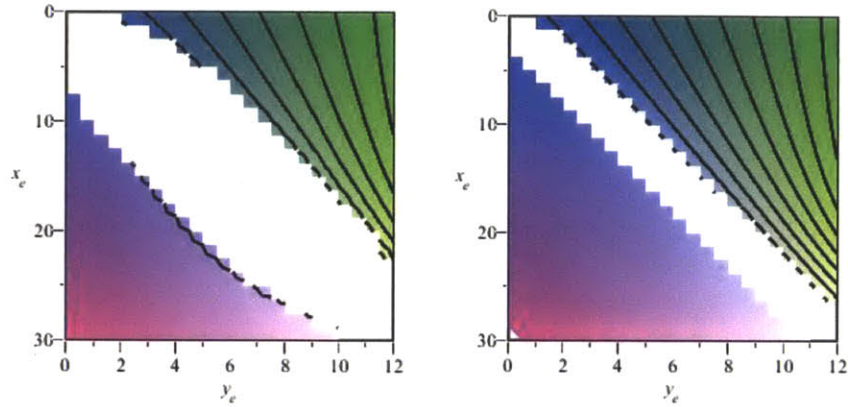
The elongation is plotted as a function of the position of E, which means as a function of both variables x_e, y_e . The maximum elongation is obtained for $x_e = 0, y_e = 12$, which means for E being at the location of B, which is equivalent to the diagonal system. When restraining the range of $x_e \in [x_{e|\min}, x_d]$, the optimum location of E becomes the one that will create the longest length for the member ED, that is to say putting E on the top member of the frame such that $x_e = x_{e|\min}, y_e = y_d$.



Figures 24 to 26: Plots of the elongation of the damper as a function of x_e and y_e . From left to right: frame of 12x20; frame of 12x30 with no constraint and with the constraint $x_e \in [15,30]$

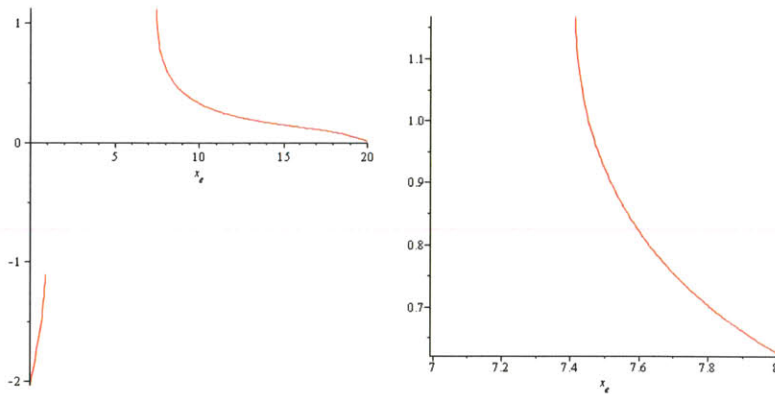
Secondly, figure 27 shows an area for which the function is not defined and this area corresponds to the diagonal of the frame and its neighborhood. This is due to our hypothesis that both members AE and EC cannot elongate; if the amplitude of the displacement exceeds that which makes AE and EC collinear, the

geometry becomes invalid. If we reduce the lateral displacement then the increase of the length of the diagonal is much smaller, so E can be closer to the diagonal. Another comment that should be made is that if the resolution of the plot was increased, then the area of non-definition of the function would decrease a little.

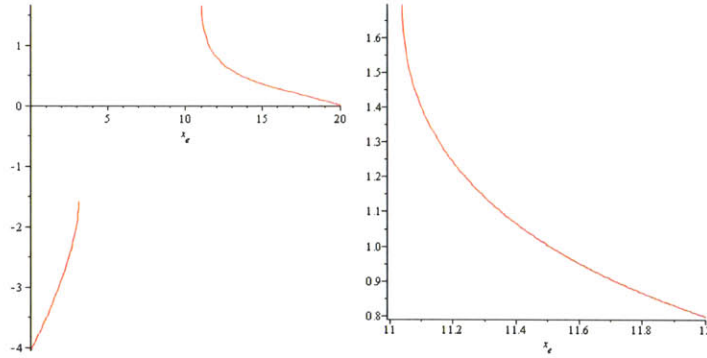


Figures 27: same plot as figure 24 but projected along the z-axis. Figure 28: same as figure 27 but for a displacement ten times smaller ($u_b = u_c = 0.05$). The lines on the surfaces represent equal elevations.

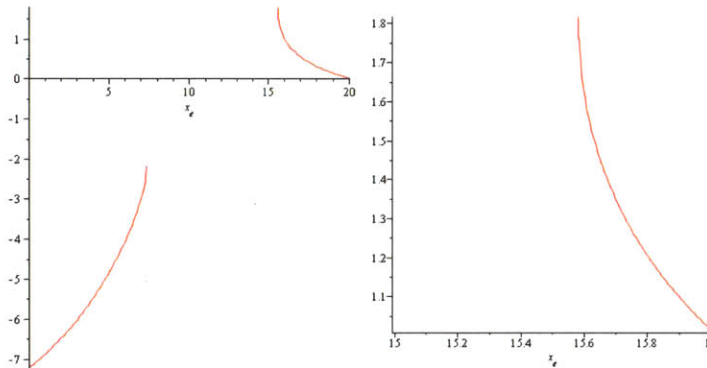
The optimization results seen above are not going to be retained as they are leading us to the configuration 1 or to an equivalent of configuration 2. Since this toggle configuration was created to differ from the first two and to have the damper on a “short” member, we are therefore going to impose a value of $y_e \neq y_d$ and optimize the position of E with regards to x_e and with the constraint that E stays in the lower triangle of the frame ACD (so only the right side of the curves should be considered). This is called the “lower” system.



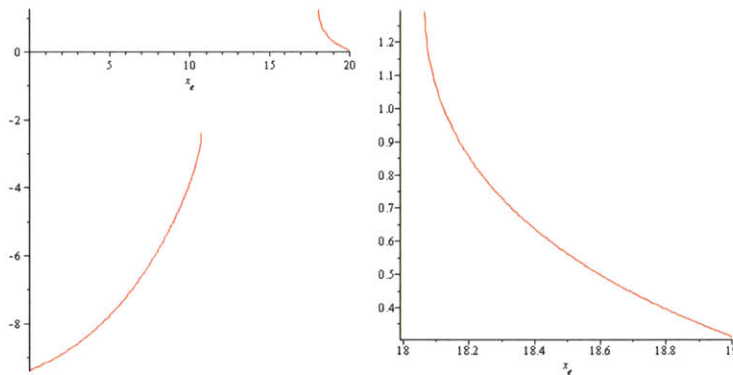
Figures 29 and 30: elongation as a function of x_e for $y_e = 2$. The optimum is found for $x_e \approx 7.45$



Figures 31 and 32: elongation as a function of x_e for $y_e = 4$. The optimum is found for $x_e \approx 11.05$



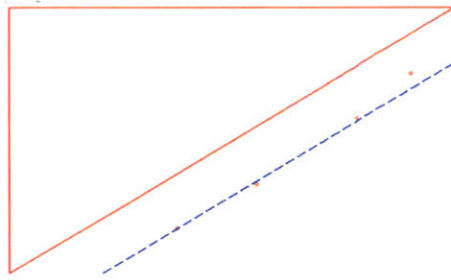
Figures 33 and 34: elongation as a function of x_e for $y_e = 7$. The optimum is found for $x_e \approx 15.6$



Figures 35 and 36: elongation as a function of x_e for $y_e = 9$. The optimum is found for $x_e \approx 18.05$

If the frame 30ftx12ft is drawn along with the results of the optimization, two major comments can be made. First of all the optimal positions of E appear to all be on the blue line which is parallel to the diagonal of the frame (the linear regression does not fit perfectly as solved $x_{e|opti}$ was solve graphically).

The optimization calculations were then conducted a second time, for the same given values of y_e but for $u_b = u_c = 0.1$ instead of $u_b = u_c = 0.5$.

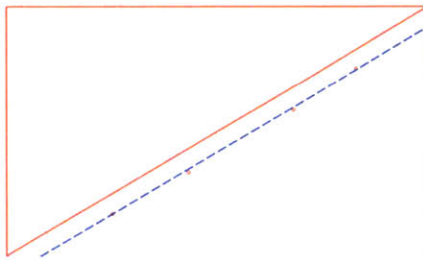


Equations of the diagonal
and the blue line:

$$(AC): y = 0.6x$$

$$(blue): y = 0.6x - 2.5$$

Figure 37: Representation of the frame 12x30 and the results of the four examples for which y_e was given and $x_{e|opti}$ was found graphically.



Equations of the diagonal
and the blue line:

$$(AC): y = 0.6x$$

$$(blue): y = 0.6x - 1$$

	$x_{e opti}$	y_e
E1	5	2
E2	8.6	4
E3	13.55	7
E4	16.55	9

Figure 38: Same examples as before but for $u_b = u_c = 0.1$ instead of $u_b = u_c = 0.5$. The table gives the coordinates of the different locations of E studied.

If the optimization problem is solved the other way round, solving for $y_{e|opti}$ for a given x_e , then the results also fit the blue line. For example, for $u_b = u_c = 0.5$ and $x_e = 10/6$, the optimal locations are E1(10;3.5) and E2(14;6).

The conclusion that can be drawn from these results is that the optimal location for E is on a parallel to the diagonal of the frame, as close to the diagonal as possible (taking into account the fact that the members AE and EC are rigid). Therefore the engineer in charge of the design needs to know which maximum perturbation is likely to occur, and this will give him the interval where the elongation is not defined and therefore the ideal location of E.

2. Influence of lateral displacement

For this case study the influence of lateral displacements, ranging from 0 to 5% of the height of the frame (5% of 12=0.6), will be studied on a frame 20ftx12ft.

As the location of E has a great influence on the results, the results are given for five different E. E1(16,2) has been chosen randomly, with the constraints that it did not have any special geometrical properties and was close enough to D (as on reference pictures of existing toggle dampers it appears that E is relatively close to D). E2(16,3) has been chosen close to E1 but slightly different to see how much the results would change for a small variation in the location of E. E3(16,7.3) corresponds to the optimal location of E for the same x-coordinate as E1 and E2 to see what would be the curve of the optimal design. E4(17,5) has been chosen so that (ED) is perpendicular to the diagonal of the frame (AD); this is a particular geometrical design of the damper that is interesting to study as it will be seen in configuration 4 that the damper should be placed perpendicular to the diagonal. E5(17,7.1) has been chosen so that (AE) is perpendicular to (ED) which is a design commonly seen in studies of toggle dampers. The figure underneath represents all those different locations.

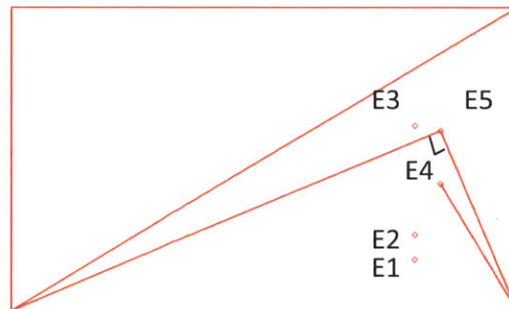
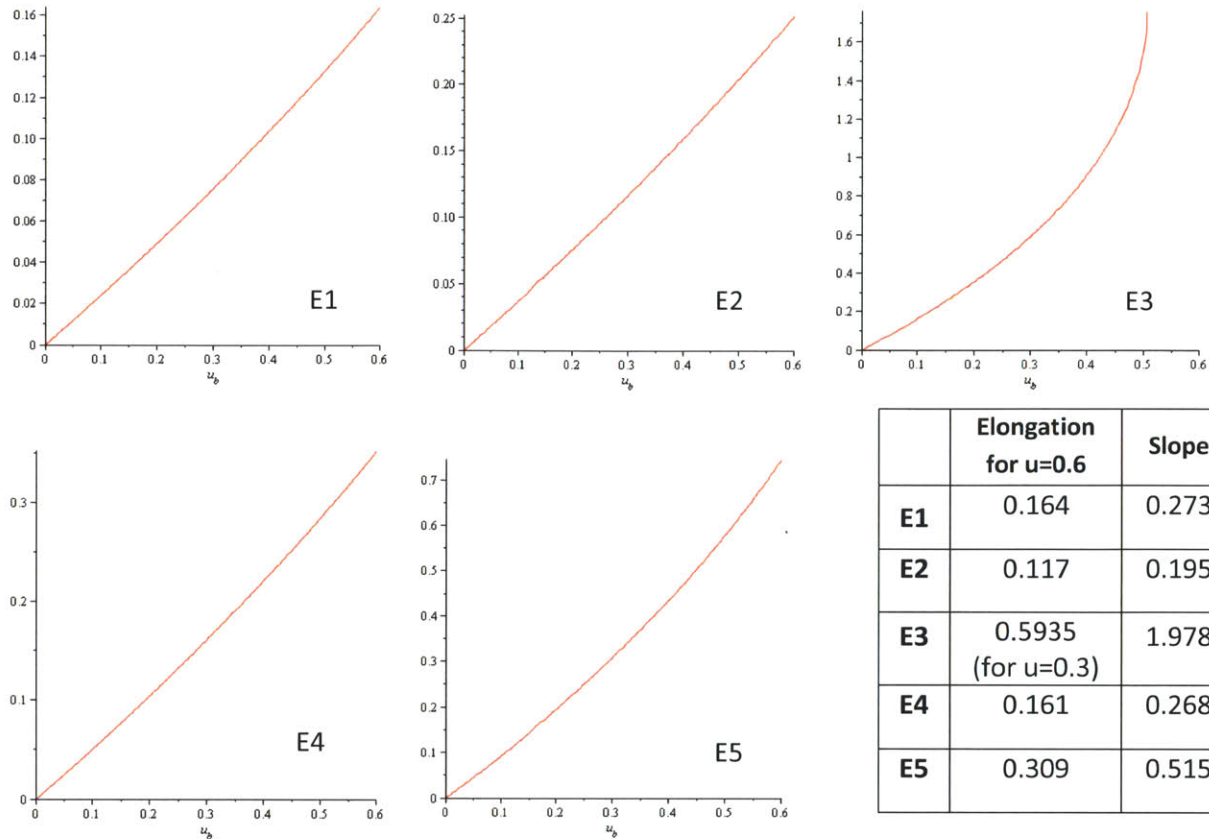


Figure 39: representation of the 5 different locations of E studied

The results show that the elongation varies nearly linearly (if we omit the case of E3), although it seems to be actually a convex function. This convexity is a good thing as for the general optimization problem studied in the second part of this thesis we will have to use the relationship between elongation and drift, and solving an optimization problem is easier with either linear or convex functions. The curve of E3 is quite different as it has a linear part until $u_b = u_c \approx 0.3$, and is undefined above $u_b = u_c \approx 0.5$ which means that in reality E is located too close to the diagonal to be able to respect the constraint of rigid members for large lateral displacements.



Figures 40 to 45: elongation as a function of u_b for different locations of E and calculations of the slope for the approximation of e as a linear function of u_b

From these results we can draw the conclusion that any random positioning of E deeply affects the efficiency of the damper which was predictable. We can also note that there is no advantage in choosing E such that (ED) is perpendicular to the diagonal of the frame. If the optimum positioning (E3) cannot be achieved, it seems that the idea of locating E such that (AE) is perpendicular to (ED) seems to be a good compromise; the slope of E5 is indeed nearly twice the one of any random positioning of E, but nearly a fifth of the slope of the optimal design. As a conclusion, for lateral displacement the toggle configuration should be either used in the optimal positioning seen in the case study 1 or such that (AE) is perpendicular to (ED). This second solution has also been studied by scholars in the configuration shown underneath.

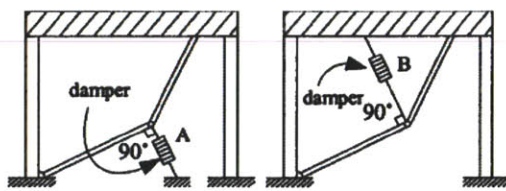
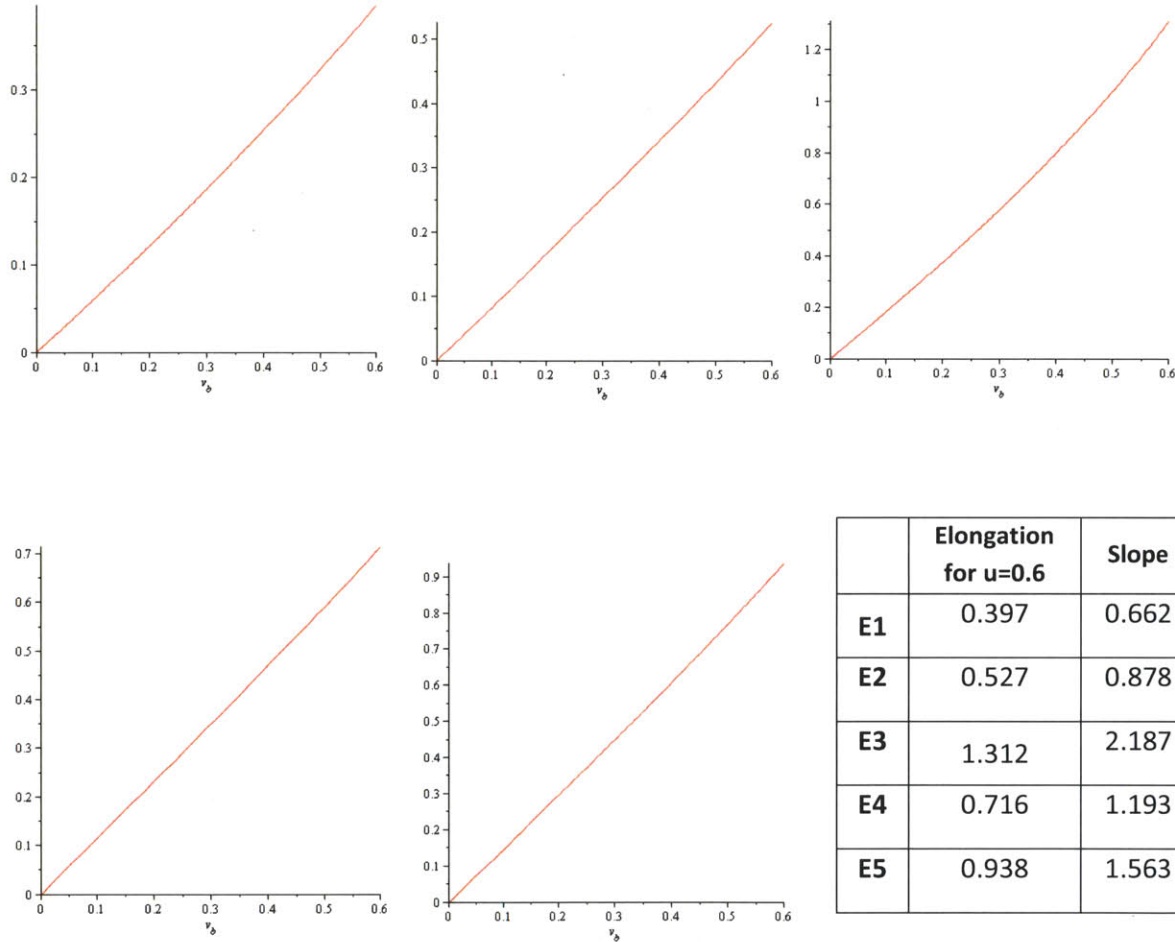


Figure 46: illustration of toggle-brace damper configuration with an angle of 90°, in the lower (left) and upper (right) systems (Constantinou et al. 2001, cited in « Analytical and Experimental Study of Toggle-Brace-Damper Systems” by J. Hwang, Y. Huang and

Y. Huang, in *Journal of Structural Engineering*, Vol. 131, No. 7, July 2005).

3. Influence of vertical displacement

The case study 3 is based on the same model as the case study 2: v_b ranges from 0 to 5% of the height of the 20ftx12ft frame and 5 different locations of E are taken into account. These are the same as previously: E1(16,2), E2(16,3), E3(16,7.3), E4(17,5) and E5(17,7.1)).



Figures 47 to 52: elongation as a function of v_b for different locations of E and calculations of the slope for the approximation of e as a linear function of v_b

The first thing that should be noted is that this configuration is very efficient for vertical displacement and keeps a linear behavior, for all 5 possible locations studied for E. This is a very different behavior than the one encountered for the other three configurations.

Secondly, it appears that the conclusions are very similar to the ones of the case study 2. The optimal location found for E in the case study 1 is indeed the most efficient design, followed by the case where (AE) is perpendicular to (ED). This time however it seems that the case when (ED) is perpendicular to the diagonal gives better results than any random location, although it is still less efficient than the two solutions mentioned earlier, E3 and E5.

4. Lateral versus vertical displacement

The comparison of both case studies 3 and 4 is given in the table underneath. It can be seen that in all cases except the optimal design, the response to vertical displacement is much better than for horizontal displacement. Secondly, it can be observed that for both types of perturbations the optimal design gives much better results than any other design and that it works nearly as well for a vertical displacement than for a horizontal one. Finally, linear relationships between the elongation and the different types of displacements can be drawn, but since the multiplicative factor depends on the location of E in a non-explicit way, a general numerical formula cannot be given.

	Slope for vertical displacement	Slope for horizontal displacement	Relative difference between slopes for a same E
E1	0.662	0.273	142%
E2	0.878	0.195	350%
E3	2.187	1.978	11%
E4	1.193	0.268	345%
E5	1.563	0.515	203%

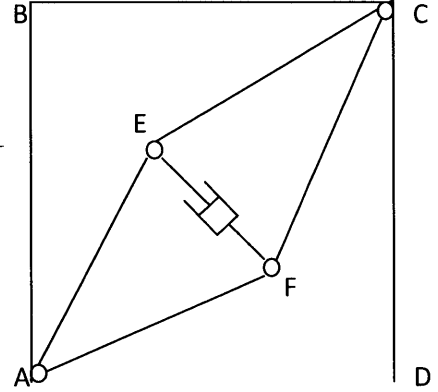
D. CONFIGURATION 4: THE SCISSOR-JACK TOGGLE SYSTEM

The steps and the equations are similar to both previous cases, but with four unknowns instead of two: u_e, v_e and u_f, v_f .

The elongation is given by:

$$e = \sqrt{(x_E + u_E - x_F - u_F)^2 + (y_E + v_E - y_F - v_F)^2} - \sqrt{(x_E - x_F)^2 + (y_E - y_F)^2}$$

The method to find the unknowns u_e, v_e and u_f, v_f is the same as before and uses the assumption that both members (AE,EC) and (AF,FC) respectively are rigid and cannot elongate. The system is the same in both cases but the values of the substitution symbols differ.



$$\Rightarrow \begin{cases} u_E = -v_E \xi + \varphi \\ v_E^2 (1 + \xi^2) + 2v_E (\beta - \varphi \xi - \alpha \xi) + \varphi^2 + 2\alpha \varphi + u_A \gamma + v_A \delta = 0 \end{cases}$$

The elongation can then be calculated.

Sensitivity analysis

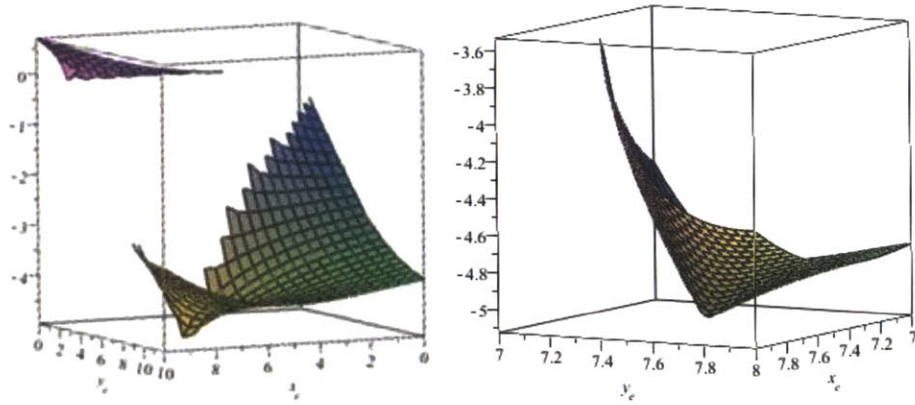
The study of this configuration will be carried out by first seeking the optimal design of this configuration, as it was done for configurations 2 and 3. Once the optimal positions for E and F will have been determined, horizontal and vertical displacements will be applied to the structure.

1. Optimum position of E when a given F

In this first set of numerical examples the optimal position of E when F is given is targeted. All examples will be given for the frame 20ftx12ft and the lateral displacement $u_b = u_c = 0.5$. To achieve this optimization, F is given a random initial position and then the elongation is plotted as a function of the

position of E, $e = f(x_e, y_e)$. The maximal absolute elongation gives the optimal position of E, for a given position of F.

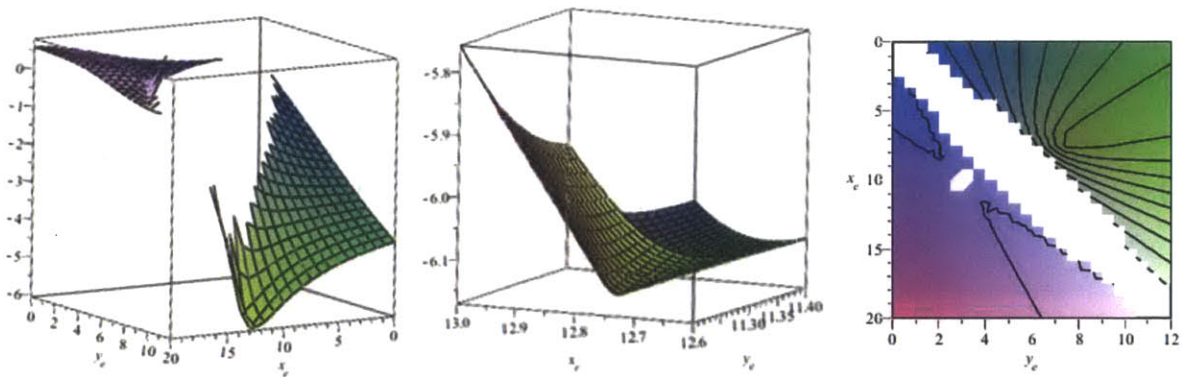
Example 1: F(10,3)



Figures 53 and 54: Elongation of the damper as a function of both variables x_e, y_e and zoom

It seems that for F(10,3), the optimal position of E is E(7.35,7.4). This seems to be very close to being perpendicular and equidistant to the diagonal of the frame, so the scalar product and distances to the diagonal are calculated. E and F are indeed symmetrical with regards to the diagonal of the frame AC.

Example 2: F(16,6)

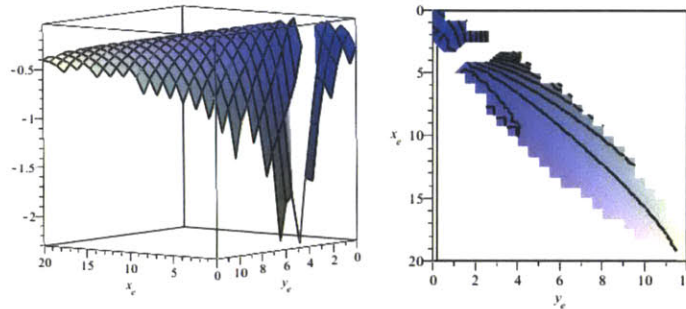


Figures 55 to 57: Elongation of the damper as a function of both variables x_e, y_e . Zoom for $x_e \in [12.6;13.0]$ and projection with contours along the z-axis.

By plotting the results, it seems that the optimal position when F(16;6) is E(12.8;11.3). Once again E and F are symmetrical with regards to the diagonal AC.

Example 3: F(4,1)

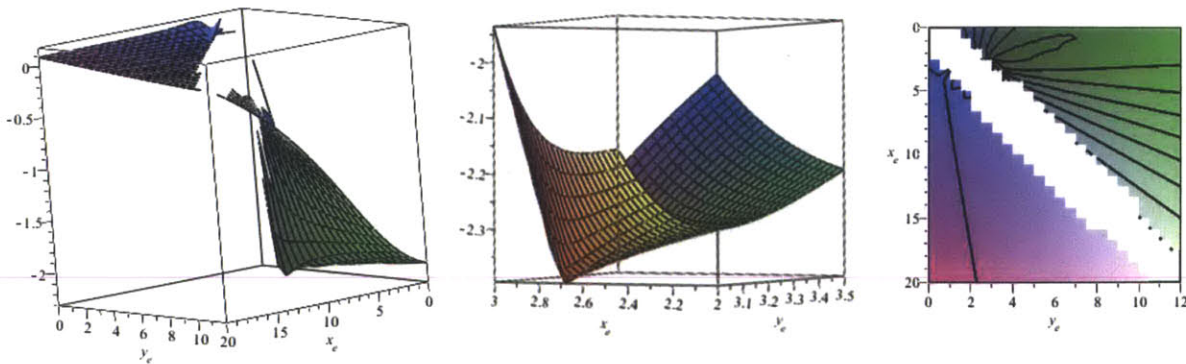
In this example, the shape of the surface plotted is from the previous ones and there is no evident maximum. In the area of the maximum elongation there is indeed a complicated surface shape. It seems to be that the optimum is found for $E(3.6; 4.4)$, which gives us: $AC.EF = -32.8 \neq 0$. As the result is unexpected and the shape very surprising, we can wonder if those results are valid. The main assumption that could be wrong is the amount of lateral displacement. Taking $u_b = u_c = 0.5$ is indeed very large, and although it allows hand-checking, real displacements should be much smaller.



Figures 58 and 59: Elongation of the damper as a function of both variables x_e, y_e and projection along the z-axis,

$$\text{for } u_b = u_c = 0.5$$

If the values are changed to $u_b = u_c = 0.1$ then the surface becomes similar to the ones of the previous examples, regular with a clear optimum. The optimal position of E is $(2.75; 3.07)$ which gives us $\overrightarrow{AC.EF} = 0.16$ (not precisely 0 as it was solved graphically) and once again E and F are symmetrical and equidistant with regards to the diagonal AC.



Figures 60 to 62: Elongation of the damper as a function of both variables x_e, y_e for $u_b = u_c = 0.1$

From left to right: complete surface, zoom for $x_e \in [2;3]$ and projection along the z-axis

Conclusion:

Different comments should be made on this first case study. First of all, the results are clearly consistent with what could be predicted, which is to say that the maximum elongation of the damper is obtained when E and F are symmetrical with regards to the diagonal of the frame AC.

Secondly, it has been seen that when a result seems inconsistent, the first thing to look at is the influence of the lateral displacement on this result. In all case studies the displacements were ranging from 0 to 5% of the height of the frame, but in reality 5% is already a large displacement that is unlikely to happen. In this configuration, if a lateral displacement is too important then the results might be wrong for two reasons. The first one is linked to the approximation of rigid members: as it has been seen in configuration 3, when the structure has rigid members in the diagonal, the function is undefined for large lateral displacements. The second reason is that what is studied are the initial positions of E and F on the deformed structure in order to obtain a condition on their positions for the undeformed structure. Therefore, if the deformed structure is very different from the undeformed one, it introduces an error in the calculation of the optimal position of E.

As E and F are symmetrical with regards to the diagonal, the elongation is only function of two unknowns instead of four. We can therefore express the elongation as a function of the unknowns u_e and v_e . The unknowns u_f and v_f are found solving the system below, knowing that the equation of the straight line

$$(AC) \text{ is: } (AC): y = \frac{y_c - y_a}{x_c - x_a}(x - x_a) + y_a.$$

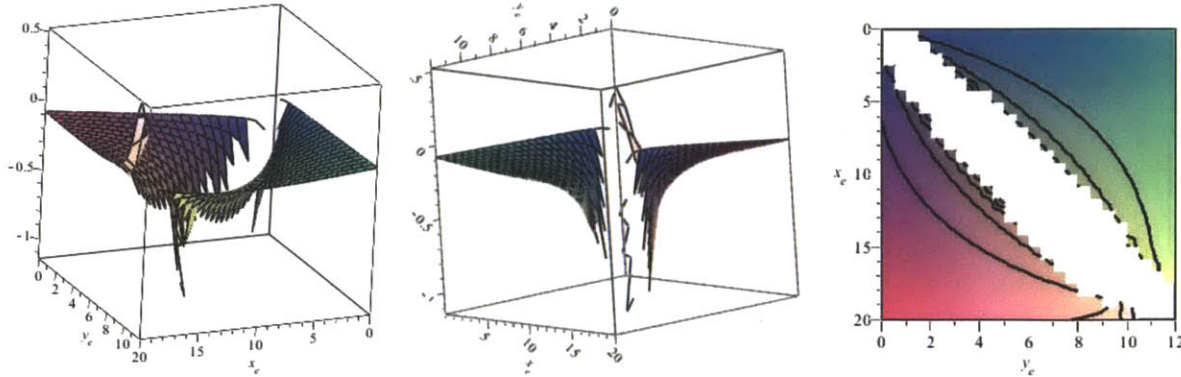
$$\begin{cases} d(E, (AC)) = d(F, (AC)) \\ \overrightarrow{EF} \cdot \overrightarrow{AC} = 0 \end{cases} \Rightarrow \begin{cases} |(y_c - y_a)x_e - (x_c - x_a)y_e + (x_c - x_a)y_a - (y_c - y_a)x_a| = |(y_c - y_a)x_f - (x_c - x_a)y_f + (x_c - x_a)y_a - (y_c - y_a)x_a| \\ (x_f - x_e)(x_c - x_a) + (y_f - y_e)(y_c - y_a) = 0 \end{cases}$$

With the assumptions that E is above (AC) and F underneath, and with A being the origin of the coordinates, we get:

$$\begin{cases} y_c(x_e + x_f) = x_c(y_e + y_f) \\ y_f = y_e - \frac{x_f - x_e}{y_c} x_c \end{cases} \Rightarrow \begin{cases} x_f = x_e \frac{x_c^2 - y_c^2}{x_c^2 + y_c^2} + 2y_e \frac{x_c y_c}{x_c^2 + y_c^2} \\ y_f = y_e \frac{y_c^2 - x_c^2}{y_c^2 + x_c^2} + 2x_e \frac{x_c y_c}{x_c^2 + y_c^2} \end{cases}$$

2. Optimal position of E and F when symmetrical

As E and F are symmetrical with regards to the diagonal (AC), the elongation is only function of the two unknowns (u_e, v_e). This second case study will therefore look at the influence of the position of E.



Figures 63 to 65: Elongation of the damper depending on the position of E, for $u_b = u_c = 0.1$. Only one half of the graph should be considered, as y_e has been plotted for 0 to 12 instead of $y_e > \frac{y_c}{x_c} x_e$. Figure 65 is the projection along the z-axis with contour

As it can be noted from the results, the elongation is maximized when E is placed near the diagonal, but the closer E and F are from the diagonal, the more difficult it is to maintain the assumption that the members AE, EC, AF and FC are rigid. This is why the function is not defined for E being too close to the diagonal. This interval of non-definition increases with the lateral displacement.

3. Influence of lateral displacement

The influence of a lateral displacement, ranging from 0 to 5% of the height of the 20ftx12ft frame, is now studied. Since the positions of E and F influence greatly the elongation of the damper, the results are given for five different positions of E and with F being symmetrical to E with regards to the diagonal.

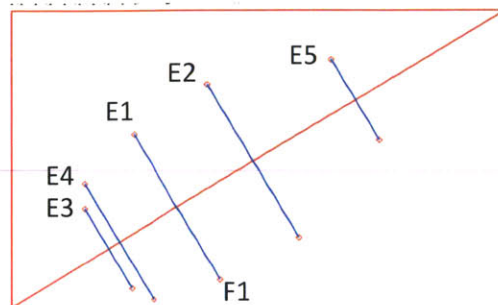
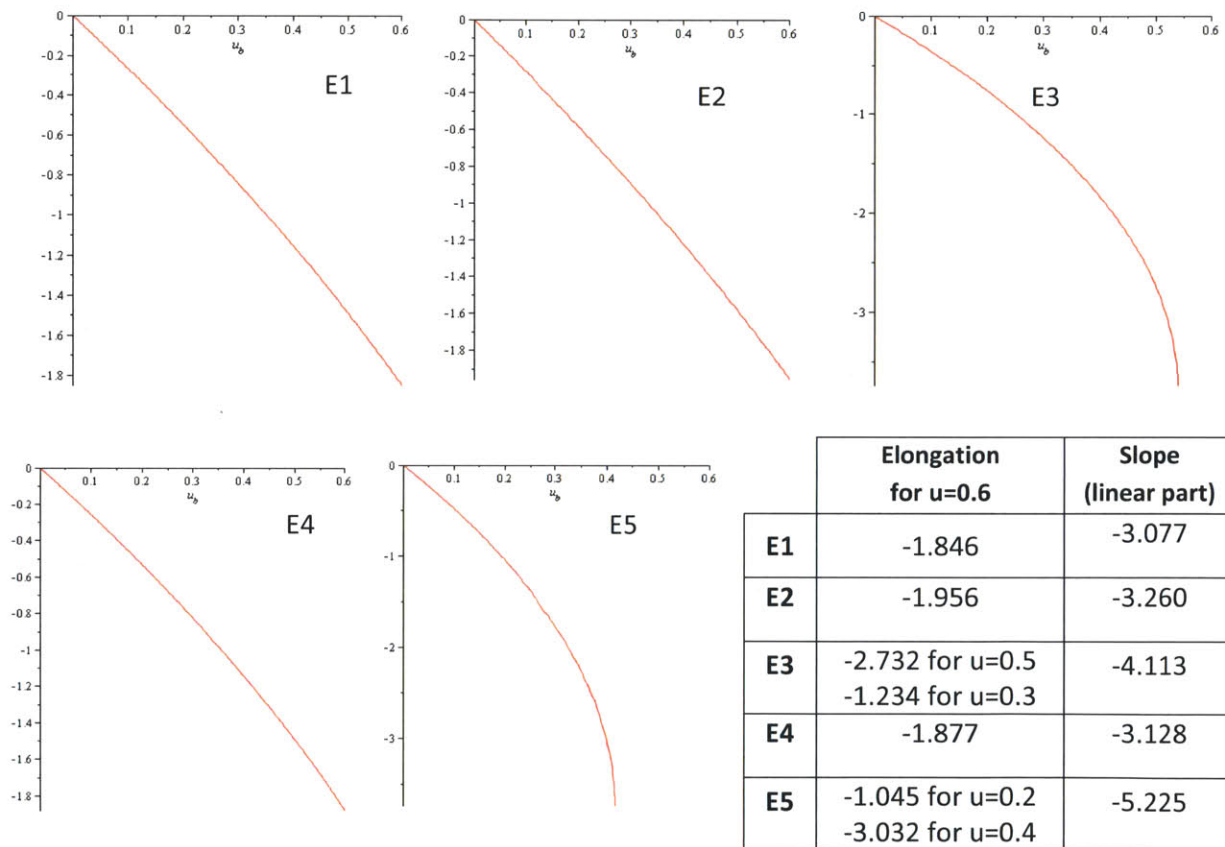


Figure 66: Representation of the frame with the different locations of E and F studied

As for E close to the diagonal there can be some issues, E1(5,7) and E2(8,9) were chosen randomly with the constraint that E be “far away” from the diagonal. However, as case study 2 also showed that the best results were obtained for E close to the diagonal, E3(3,4) was chosen close to the diagonal to see how much the elongation would increase when going for the optimal yet problematic design. E4(3,5) was chosen close to E3 but slightly further away to see how fast the issues would disappear and how much it would make a difference in the elongation. Finally, E5(13,10) was chosen as close to the diagonal as E3 but on the upper side to see if relative displacements of nodes were of influence. The results are shown underneath.



Figures 67 to 72: elongation as a function of u_b for different locations of E and calculations of the slope for the approximation of e as a linear function of u_b

First of all it can be observed that when E is far enough from the diagonal the function varies linearly, but as soon as E gets closer to the diagonal the function, which is not defined for large values of u , varies linearly until reaching an asymptote. Secondly, we can highlight the fact that for all locations the slope is unusually large, but of course it gets even more important when E comes closer to the diagonal (optimal

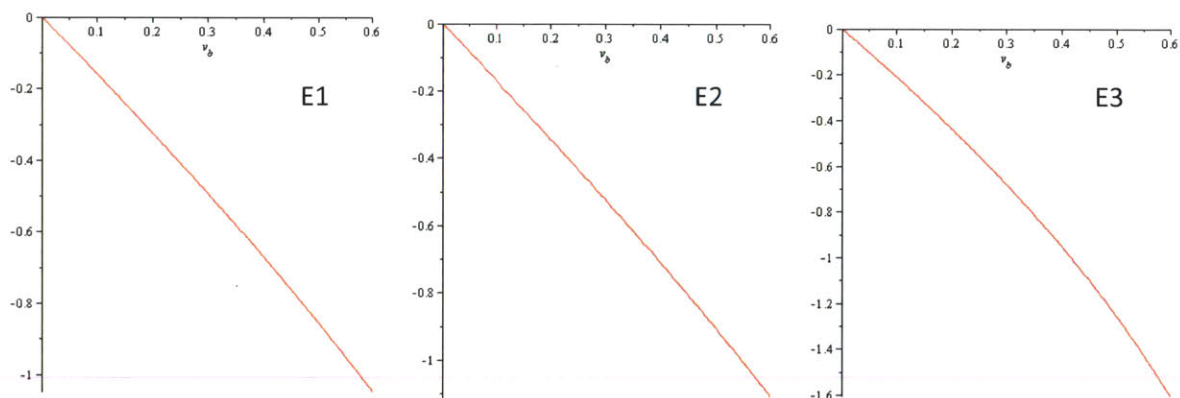
design as seen in case study 2). Thirdly, we notice that there is an important change of behavior between E3 and E4, and between E3 and E5.

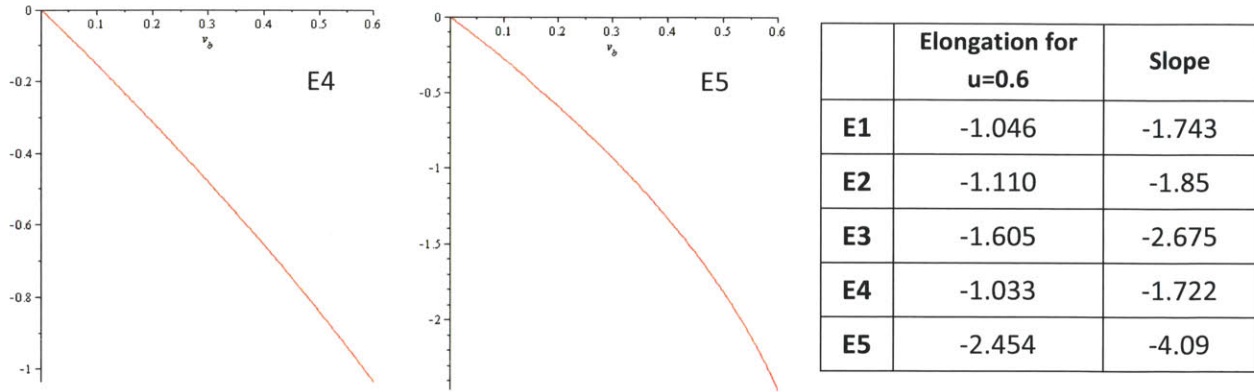
As a conclusion, we can say that this configuration is extremely efficient under lateral displacement, and that the best way to optimize it, is by:

- having E and F symmetrical with regards to the diagonal
- E "close" to the diagonal
- E "close" to the point which experiences the most relative displacement, in this case C.

4. Influence of vertical displacement

This case study was carried on a frame 20fx12ft and for the same locations of E and F as previously. In this case the slopes vary also linearly, but there are no longer issues with E getting close to the diagonal. Furthermore, the best results are obtained for E being close to the diagonal and once again, the optimum location is E5, which is both close to the diagonal and close to the corner of the frame that has the most important relative displacement.





Figures 73 to 78: elongation as a function of v_b for different locations of E and calculations of the slope for the approximation of e as a linear function of v_b

5. Horizontal versus vertical displacement

The comparative table is given underneath. This configuration works much better for lateral displacements than for vertical displacements, although being already very efficient for vertical displacements. As for configuration 3, it appears that when E is close to its optimal location then the relative difference of efficiency between the vertical and horizontal responses decrease.

	Slope for a horizontal displacement (linear part)	Slope for a vertical displacement	Relative difference between slopes for a same E
E1	-3.077	-1.743	76.5%
E2	-3.260	-1.85	76.2%
E3	-4.113	-2.675	53.8%
E4	-3.128	-1.722	81.6%
E5	-5.225	-4.09	27.8%

As a conclusion, this configuration should be used for lateral displacements. Furthermore, the optimal locations for E and F are those that were highlighted earlier:

- E and F symmetrical with regards to the diagonal

- E close to the diagonal
- E close to the point which experience the most relative displacement, in this case C.

E. CONCLUSION OF PART I

Part I examined four common damper configurations including: the diagonal system, the Chevron system, the toggle system and the scissor-jack system. Elongations were calculated without approximations for all four configurations to find their exact formula. Initially, this thesis assumed that the symbolic expressions of elongations would be easy enough to be linearized. Linearized expressions would have then been compared to approximations commonly used in civil engineering and compared to the exact expressions of the elongations, which would have enabled a better understanding of differences introduced by approximating the results. Unfortunately, the expressions calculated for the elongations were too long to be of use mathematically. Numerical case studies were therefore carried out using the exact expressions of the elongations, which enabled a better understanding of the type of results obtained for small perturbations (vertical or horizontal loads ranging from 0 to 5% of the height of the frame). Results of most numerical case studies proved that the functions varied nearly linearly. As a result, approximate linear formulas were derived which linked the elongation to the perturbation. Additionally, the optimal design for configurations 2, 3 and 4 were calculated. Detailed results may be found in the previous paragraphs.

Results obtained in part I are used in part II, which focuses on optimizing both the locations as well as the type of dampers used in buildings.

PART II - OPTIMIZATION PROBLEM

The main aim of this thesis is to optimize the positioning of dampers in a building. The inputs of this problem are: the geometry of the building, its modal shapes and the damping that is targeted for each mode. Knowing the price and the response of each type of damper, the cost of installation of dampers for the given constraints can be minimized.

There are three steps in the optimization process. The first step is the calculation of the possible elongation for each type of damper and each location. This can be obtained by knowing the displacements of the nodes for each mode and the formula of the elongation of each configuration of dampers. The second step is the definition of the costs. The cost of each damper is a function of both the type of damper used (directly linked to the allowable force of the damper) and also its location. For example, the price of any type of damper located on the façade of a building will rise to compensate for the architectural drawback of its position. The third step is the optimization in itself for given constraints. The most obvious constraint is the targeted damping for each mode, but it could also be a constraint on the numbers of dampers of type j used or on the subset locations where dampers of type j may be used for example.

The problem will first be exposed mathematically. A 2D-example will be studied to find patterns in the positioning of dampers and the resulting damping ratio achieved. This example will also be used to show how price can influence the positioning of dampers.

F. Mathematical description of the optimization process

There are three stages in the optimization process. The first phase is to calculate the possible elongation for each type of damper, for each location and for each mode. The elongations must be calculated using a linear approximation in order to use the expression of the normalized contribution of location k to the damping ratio of mode m as it is defined later. As a result, the displacements of the nodes for each mode can be directly used as the input of the linear optimization problem. Part I of this thesis addressed those calculations for four common configurations of dampers.

1. Definition of the algebraic parameters

The three first variables to be defined are K, J and M, where K is the number of possible locations where a damper can be installed; J is the number of different types of dampers that can be used; and M is the number of modes of the building to be studied. As using multiple types of dampers may lead to confusion and errors during construction, it is highly probable that J=1. In the following example J=1 for sake of simplifying the optimization problem.

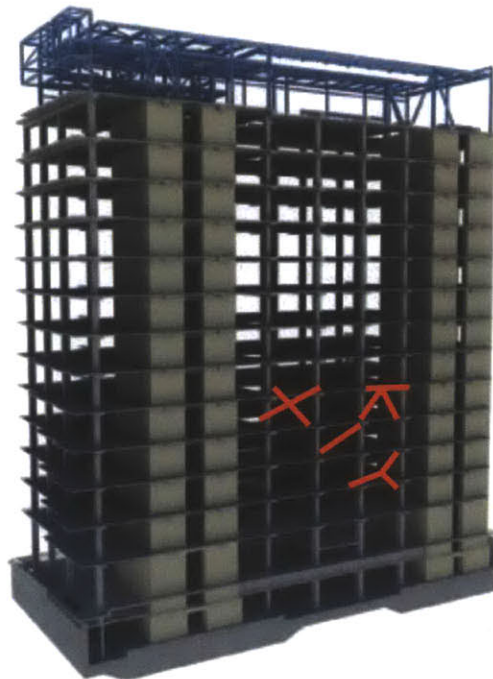


Figure 79. Illustration of how dampers of different type can be located in a building. K and J can have large values.

c_{jk}	Damping parameter of type j damper placed at location k
$e_{mk}(j)$	<p>Elongation of damper installed at location k for the mode shape m</p> <p>It is a function of j, the type of the damper. Ideally it would be expressed as: $e_{mk}(j) = \vec{F} \cdot \vec{\phi}_m$, the elongation being a linear function of the displacements of each node.</p>

k_m	Stiffness of mode m
μ_m	Mass of mode m
$\xi_{km}(j)$	Contribution to the damping ratio of mode m of the damper placed at location k. It is a function of j, the type of damper.
ξ_m	Damping ratio of mode m It can be shown that: $\xi_m = \sum_k \xi_{km} = \sum_k \sum_j \left(\frac{e_{km}^2(j)}{2\sqrt{k_m \mu_m}} \right) \cdot c_{jk} \cdot \alpha_{jk} = \sum_k \sum_j x_{km}(j) \cdot c_{jk} \cdot \alpha_{jk}$
$\xi_{m target}$	Target damping ratio for mode m. It is the minimum damping ratio that has to be achieved for mode m.
$x(j) = (x_{mk}(j))_{m \in [1, M], k \in [1, K]}$	Matrix of the normalized contribution of location k to the damping ratio of mode m. The coefficients of the matrix are given by: $x_{mk}(j) = \frac{e_{km}^2(j)}{2\sqrt{k_m \mu_m}}$. Since the elongation depends on the type of damper j used, there are actually J matrices $x(j)$.
$p = (p_{kj})_{k \in [1, K], j \in [1, J]}$	Matrix of the cost associated with placing a damper of type j at the location k.
$\alpha = (\alpha_{jk})_{j \in [1, J], k \in [1, K]}$	Matrix to be optimized. It gives the type of dampers used and the location in which they are installed. The coefficients can only take two values: 1 or 0. If $\alpha_{jk} = 1$ then it means that a damper of type j is installed at the location k, otherwise $\alpha_{jk} = 0$.

To understand the optimization problem, the most important is to understand the variable that is to be optimized: the matrix $\alpha = (\alpha_{jk})_{j \in [1,J], k \in [1,K]}$. This matrix contains all the information to position the damper in the optimal way as it gives the type of damper used and in which location. Since it is made of binary coefficients, it is more difficult to use. Solving an optimization problem for integers is indeed more complicated than solving on a continuous range of real numbers.

Secondly, the formula that is interesting to note because it links Part I to Part II of this thesis is:

$$\xi_m = \sum_k \xi_{km} = \sum_k \sum_j \left(\frac{e_{km}^2(j)}{2\sqrt{k_m \mu_m}} \right) \cdot c_{jk} \cdot \alpha_{jk} = \sum_k \sum_j x_{km}(j) \cdot c_{jk} \cdot \alpha_{jk} \quad \text{with: } x_{mk}(j) = \frac{e_{km}^2(j)}{2\sqrt{k_m \mu_m}}$$

It indeed shows how the elongation of a damper is related to the damping ratio of the mode m of a structure. As the optimization problem is set to find the locations and types of dampers to use in order to get the minimum cost while achieving a targeted damping ratio, it explicitly shows the use of the results obtained in Part I.

2. Definition of the problem

The general problem can be written as:

Determine the matrix $\alpha = (\alpha_{jk})_{j \in [1, J], k \in [1, K]}$ that minimizes the cost of the installation of dampers:

$$Cost = \sum_k \sum_j p_{jk} \alpha_{jk} = Tr(P\alpha)$$

Knowing that the constraints are:

- the damping ratio of each mode needs to be superior to the target damping ratio

$$\sum_k \sum_j x_{mk}(j) \cdot c_{jk} \cdot \alpha_{jk} \geq \xi_{m|target}$$

- there can only one type of damper at each location at the maximum

$$\sum_j \alpha_{jk} \leq 1$$

A few comments need to be made on this mathematical description of the problem. First, if it is assumed that a single type of damper type of damper can be used, then the problem is simplified to:

- $J=1$

- Determine the vector $\alpha = (\alpha_k)_{k \in [1, K]}$ that minimizes the cost of the installation of dampers:

$$Cost = \sum_k p_k \alpha_k = P^T \alpha$$

- Knowing that the constraints are:
$$\begin{cases} \sum_k x_{km} c_k \alpha_k \geq \xi_{m|target} \\ \alpha_k \in \{0,1\}, \forall k \in [1, K] \end{cases}$$

Secondly, the damper capacity c_{jk} must be previously calculated. This will either lead to an exact result

or to another set of constraints: $c_{jk} = \frac{F_j}{v_k}$ or $c_{jk} < \frac{F_j}{v_k}$, where v_k is the design velocity at the

location k (which can be obtained by seismic analysis) and F_j is the capacity of the dampers of type j . It

is to be kept in mind that the price of dampers is a function of the force F_j . Thirdly, as seen in the

general case, the trace of a matrix must be minimized; this problem is written in an unconventional manner for solving linear problems. To remedy this issue, a vector $\alpha' = (\alpha'_l)_{l \in [1,JK]}$ that combines the vectors collected from each line of the matrix $\alpha = (\alpha_{jk})_{j \in [1,J], k \in [1,K]}$ is created, meaning that α' will first contain all the information of the damper of type J=1, then those of the damper of type J=2, etc.

As a fourth remark, complications arise from the dependency x_{mk} has on j. It indeed means that there are J matrixes $x(j) = (x_{mk}(j))$ to be created, each one giving the elongation for each mode and each location for the type j damper. Then, to calculate the damping ratio of mode m, the program needs to run through all the J matrixes to find the values that will achieve the constraint:

$\sum_k \sum_j x_{mk}(j) \cdot c_{jk} \cdot \alpha_{jk} \geq \xi_{m|target}$. The complication arises from the fact that there is not a single matrix to fetch the values from.

G. 2D- Example: linking location of dampers and damping ratios achieved

A 2D-example is studied to demonstrate uses for and results from this optimization process. Although a 2D-structure will not have the same behavior as a 3D-structure, it creates an interesting asymmetrical structure with a reasonable number of possible locations, making it easy to interpret and check if the results are coherent.

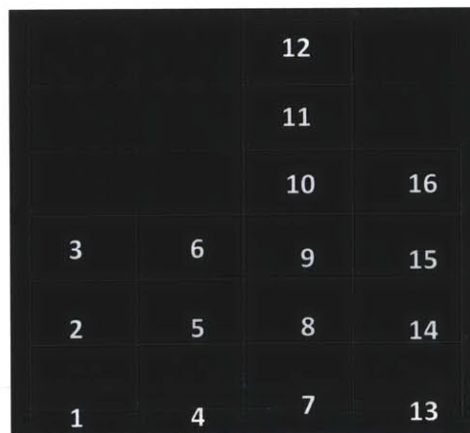


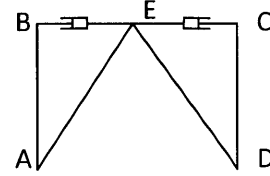
Figure 80: The 2D-asymmetrical structure studied and the K=16 possible locations for dampers. W12x40 sections were used for all beams and W10x33 for all columns

There are 33 nodes and 16 possible locations to install dampers in this structure. In order to simplify this example and see how the positioning of the dampers influences the other modes, the optimization has been carried out for one single type of damper: the chevron brace in its optimal configuration (E being in the middle of the top member as seen in the first part of this thesis). The elongations have been calculated using the approximate formulas for a lateral displacement:

$$e_1 = l_{final} - l_{initial} \approx (x_e + u_a - x_b - u_b) - (x_e - x_b) = u_a - u_b$$

$$e_2 = u_c - u_d$$

$$e_{km} \cong e_{total} = \sqrt{e_1^2 + e_2^2}$$



As seen earlier, the use of one single type of damper simplifies greatly the problem which can be therefore solved using a linear solving function of Maple that uses the branch and bound method. In order to see the relative efficiency of each damper, the vector $\alpha = (\alpha_k)_{k \in [1, K]}$ calculated by Maple has values ranging from 0 to 1, 1 meaning that the damper in this location is used to its maximum capacity. The vector $\alpha = (\alpha_k)_{k \in [1, K]}$ was then translated into the optimal vector $\alpha_{opt} = (\alpha_{k,opt})_{k \in [1, K]}$: if $\alpha_k \in]0, 1[$ then $\alpha_{k,opt} = 1$, else $\alpha_{k,opt} = \alpha_k$; and the damping ratios were calculated for α_{opt} . In reality a damper is either installed at location k or not, so that α_{opt} represents reality, but α shows how much of the maximum efficiency of the damper is actually used, 1 meaning that it is used to its maximum capacity.

The structure has been modeled on SAP in order to get the shapes of the first twelve modes and the displacements of each node for each mode. Since earthquakes are mostly exciting the horizontal modes, the first six modes are those that should be taken into account according to the mode shapes presented on next page. Mode 12 could also be taken into account but its frequency is so small compared to the first ones that it does not really matter.

For this first example the prices P were set equal to 1 and the damping parameters were also set to a single constant that was varied to see how the damping optimization changed. This was made in order to study the possible links between the location of dampers and the damping ratios achieved. To do so, the targeted damping ratios were changed so that one single mode would be studied or several ones. The values of c are not representative of real damper capacities but are being changed in order to increase or reduce the number of dampers needed to achieve the targeted damping ratios. If c is too small, the optimization problem has no solution, but if it is taken too big, then only one damper is usually needed for the whole structure. The complete results of the case studies are given in Appendix 5.

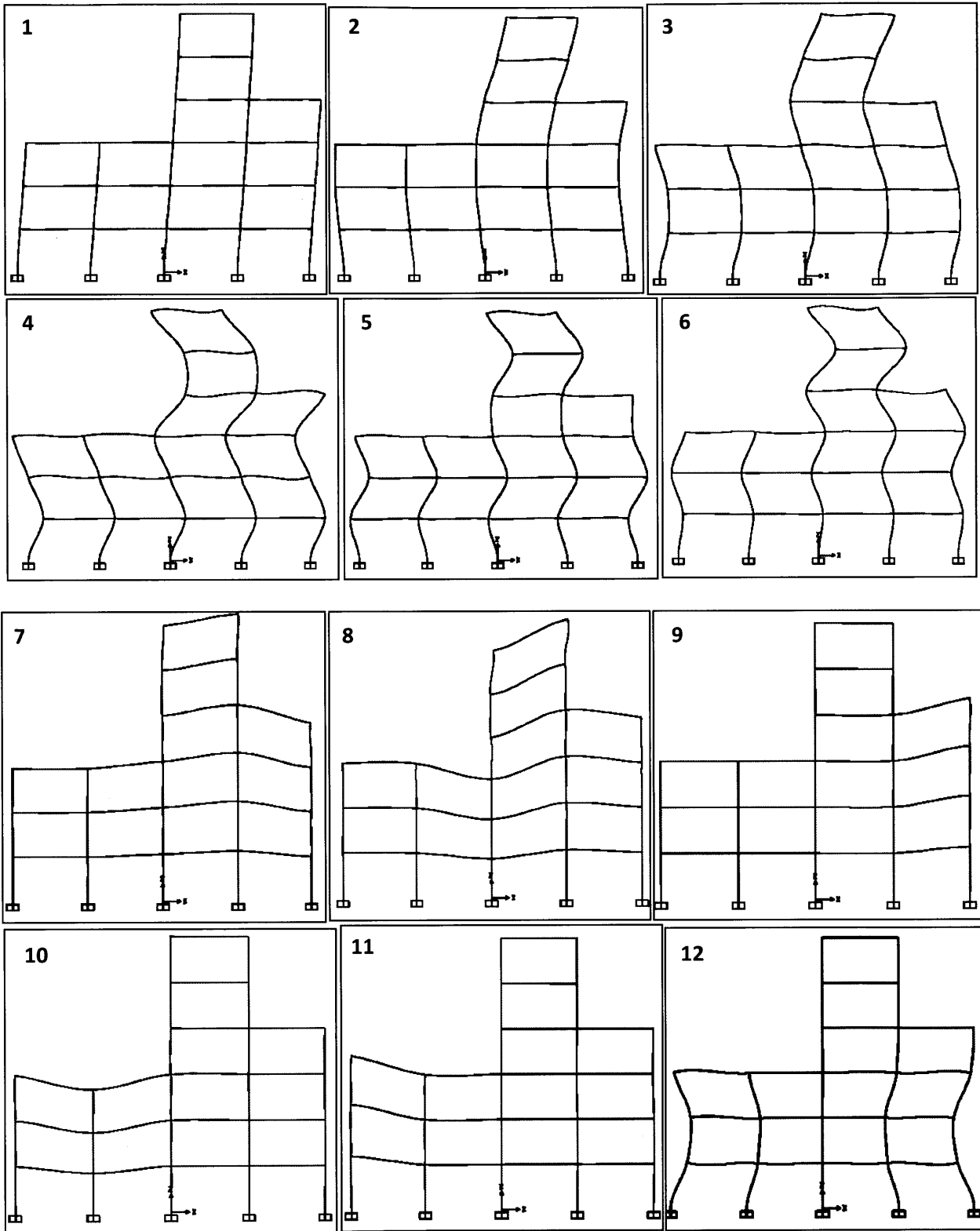


Figure 81: From left to right and top to bottom: the shape of the first twelve modes of the 2D-structure

1. Damping ratio target for mode 1 only

The optimization problem is first solved by only imposing a constraint on the target damping ratio of mode 1. When requiring $\xi_{1|target} = 5\%$, the boundaries of c are as follow: for $c \leq 0.3$ the optimization problem has no solution and for $c = 5$ a single damper is installed. This gives us an approximate range of values of c that will be used throughout the study of this 2D-example. Knowing the top boundary of c , the value of c is slowly decreased until reaching its lower boundary, so that dampers are added one at a time and so that the most efficient locations for damping mode 1 can be identified. The order of efficiency of the locations is the same for all $\xi_{1|target}$ and all c , but the values of the achieved ξ_m are different. Sometimes the resulting ξ_m is way too large to have a real significance, but is nonetheless useful for reasoning in terms of importance and ratios between ξ_m .

In this case, it appears that if only one damper has to be installed to damp mode 1, it should be in location 2. The most important locations are then, by order of importance: 5, 8, 14, 10 and 16. If two more dampers were to be added it would be in locations 9 and 15, and a third one could be put in location 11. Finally, by decreasing even more the value of c , the locations 3 and 6 are to be used along with those on the first floor. Surprisingly the location 12 is not taken into account unless $\xi_{1|target} = 20\%$ and $c = 1.5$. It can also be noted that dampers are usually positioned on the whole floor before moving on to another floor. The exceptions, the third floor in this case study for example, are due to the asymmetry of the building's geometry.

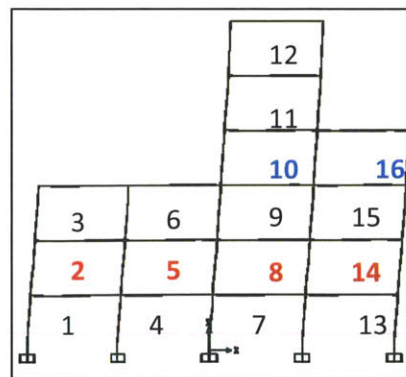


Figure 82: shape of mode 1 and the 16 possible locations for dampers. For ease of reading, the red numbers represent the most efficient locations and the blue ones the secondary locations.

The first mode of an idealized structure would be perfectly linear, meaning that the drift ratio would be constant so that every location would be equivalent. Nonetheless, as it appears not to be the case, one can wonder why location 2 is the most efficient one instead of location 12 for example. This result is specific to this example and to the way the elements were modeled on SAP. In a real 3D structure, with different types of columns and beams, the behavior might change completely and the most efficient location might be at the top of the building for example.

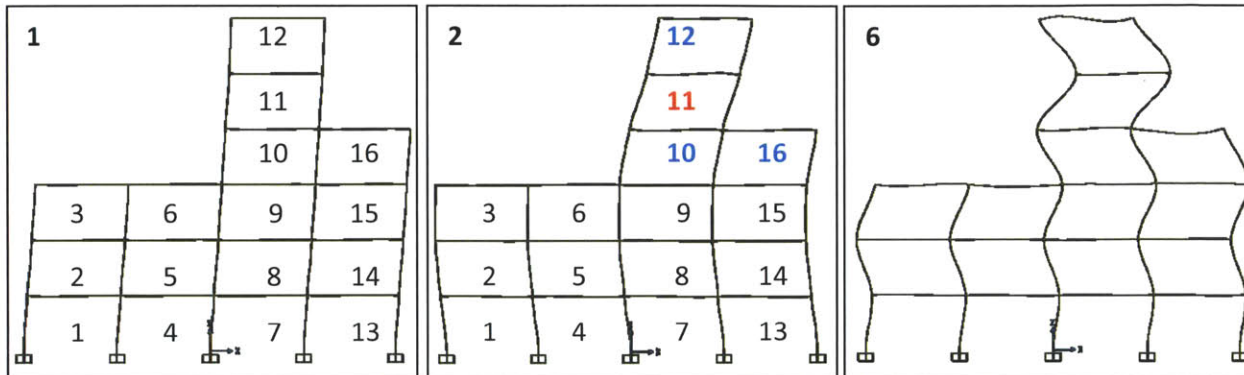
The achieved damping ratios are also interesting to study. It appears that they are increasing from mode 1 to 5 (or 6) as long as there are several dampers (at least 8). Although it was expected, it is a very interesting result. Looking at the shape of the different modes, it seems that positioning dampers on the 2nd floor should not influence many modes apart from modes 5 and 6. This explains why the damping ratios are not increasing when there are only a few dampers -as they are first positioned on the 2nd floor- and why mode 5 is so well-damped in those cases (the difference between modes 4, 5, 6 could not be predicted with the mode shapes and would have necessitated the use of the drift ratio).

Lastly, several comments are to be made on the relations between damping ratios. First of all, it appears that $\xi_2 \geq 1.5\xi_1$ when dampers are located on several floors. Secondly, mode 5 is often the one with the maximal damping ratio and the relation $\xi_5 \geq 3\xi_1$ is always verified. The damping ratio of mode 6 is more complicated to analyze as its behavior with regards to ξ_5 is unclear, but it is apparent that it is always superior to ξ_3 and that it is either superior to or of the same order of magnitude than ξ_4 . Lastly, without surprise, it can be seen that modes 7 to 11 are not damped and that mode 12 may be a little damped, but no more than $\xi_{12} \leq \frac{\xi_1}{3}$.

2. Damping ratio targets for modes 1 and 2

The response of the structure is first studied when the only constraint is on the damping ratio of mode 2. By order of importance, the dampers have to be placed in location 11 then 12 then 10 then 16 and then on the 1st floor. It is logical that the dampers have to be placed on the asymmetrical top part of the structure to damp this mode, but it is surprising that location 11 is more efficient than location 12. If a unique damper is positioned in the structure in location 11, then it appears that modes 2 and 6 are

highly-damped, modes 3 and 5 are medium-damped, mode 1 is very little damped and all others are not damped at all. If a second damper is then added in location 12, the damping ratios of modes 3, 4 and 5 increase significantly but mode 2 seems to be unaffected. This corroborates the fact that location 11 is more efficient for the damping of the second mode than location 12, although it is not obvious when looking only at the shape of mode 2 and not the drift ratio.



Figures 83 to 85: From left to right, the shape of modes 1, 2 and 6 and the possible locations for dampers

By looking more closely at the values of the damping ratios attained, it can be seen that if there are more than two dampers then the damping ratios increase from ξ_1 to ξ_6 , with the exception of ξ_5 which has a changing behavior. Also, mode 1 is such that $\xi_1 \leq 5\%$ even when $\xi_{2|target} = 20\%$. Finally, there is no mode which is abnormally damped compared to the others.

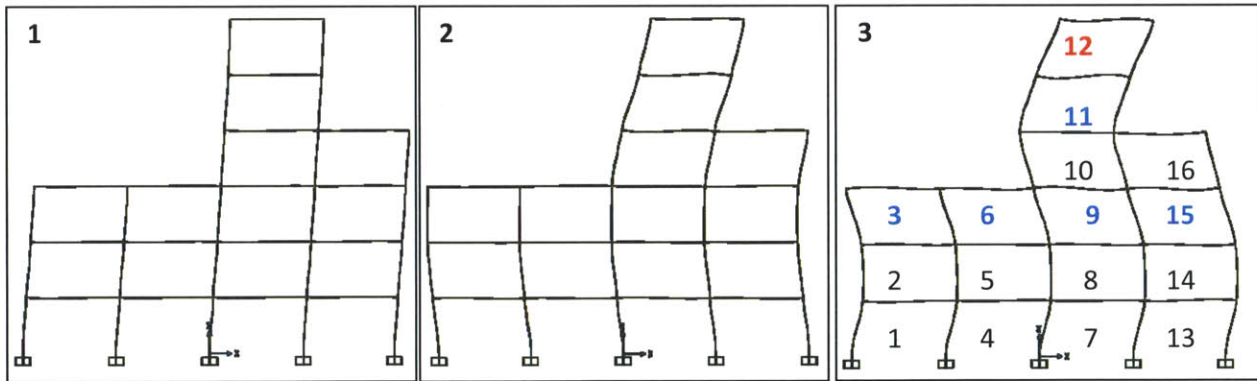
This leads us to study the case when a damping ratio is targeted for both modes 1 and 2. As seen earlier, the most important location for mode 2 is n°11 and those of mode 1 are, in order of importance: 2, 5, 8 and 14. It is therefore without surprise that to achieve targeted damping ratios of $\xi_{1|target} = \xi_{2|target} = 20\%$ dampers have to be positioned on the 2nd floor and at location 11. By increasing the value of c, only two dampers have to be used, located at positions 2 and 11. However, this solution is not realistic as the damping ratios attained are absurdly high, but it is nonetheless interesting to be noted. Another point which is of interest is the unusual values of the vector α . In general there is only one value of α_k which is such that $\alpha_k \in]0,1[$ and then, by increasing the value of c the damper k is no longer needed. In this case, there are always two α_k which are such that $\alpha_k \in]0,1[$, one of them being 11. Although $\alpha_{11} < \alpha_k$, meaning that the contribution of damper in location 11 is very small, it is

the damper from location k that disappears when increasing c. This is a perfect example showing how specific locations can be with regards to the damping of a particular mode.

Lastly, when damping ratios are targeted for both first modes, it seems that no general rule of increase can be observed, but apart from mode 3, it appears that the damping ratios of modes 2, 4, 5 and 6 are systematically higher than ξ_1 , to the point where modes 5 and 6 are 100% damped.

3. Damping ratio targets for modes 1, 2 and 3

The behavior of the structure is first studied when only mode 3 is targeted for an optimal damping ratio. The locations which are the most efficient to damp mode 3 are, by order of importance: 12, 11 and those on the 3rd floor. It appears that this positioning affects mostly modes 3, 5 and 6, which damping ratios are of the same order, and very little mode 1 which damping ratio barely reaches 3% although $\xi_{3|target} = 20\%$.



Figures 86 to 88 : From left to right, the shape of modes 1, 2 and 3 and the possible locations for dampers

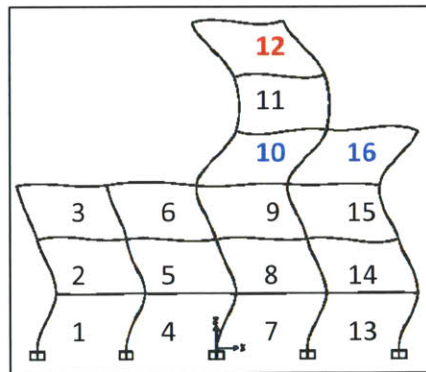
If the optimization problem is made more complicated by requiring $\xi_{1|target} = \xi_{2|target} = \xi_{3|target} = 20\%|30\%$, then two dampers at the minimum are needed, even for values of c which are way too high to be realistic. These have to be positioned at locations 2 and 11, as for the previous case study of the coupling of modes 1 and 2. It is only for small values of c (when 7 dampers at least are needed) that there is a change in the behavior of the structure with regards to the previous case study, but it is not even significant as for another small decrease of c it appears that all locations need to be occupied. Furthermore, the general behavior of the damping ratios, except when

only when only few dampers are needed, is to increase with the modes, reaching extremely high values for modes 4, 5 and 6 (over 90% for $c=3$ and a target of 30%).

As a result, it should be remembered that targeting a value for mode 3 has little impact on this 2D-structure. Since the damping ratios tend to increase with the modes, the targeted values for $\xi_{1|target}, \xi_{2|target}$ is what defines the result of the optimization process if $\xi_{1|target} = \xi_{2|target} = \xi_{3|target}$.

4. Damping ratio targets for modes 1, 2, 3 and 4

As for the previous case studies the mode 4 alone is first studied. It appears that the location the most efficient is n°12 and then comes both locations n°10 and n°16. If more dampers have to be added, they will be located on the 3rd floor on the left-hand side and on the 2nd floor on the right hand-side. The first remark is that obviously mode 4 corresponds to the limit of which modes start to have complicated shapes. There are no obvious relationships between damping ratios that can be derived from the results, and it seems that in general the only well-damped mode is mode 4. The damping ratio of mode 1 stays around 1% -2%.

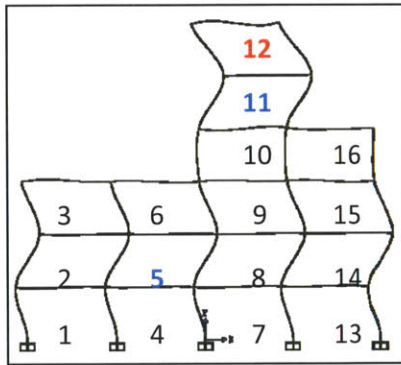


Figures 89: the shape of mode 4

For a constraint such as $\xi_{1|target} = \xi_{2|target} = \xi_{3|target} = \xi_{4|target} = 20\%|30\%$ the optimization results are exactly the same as in previous cases. This is due to the fact that the damping ratios tend to increase, and even if modes 4 and 5 have sometimes unexpected values, these are usually always higher than the first two modes, so by giving a constraint on the first two modes the following modes will be fine.

5. Damping ratio targets for modes 1, 2, 3, 4 and 5

As previously, mode 5 alone is first studied. The most efficient locations are: 12 then 11 then 5. This leads us to look into more depths at the results for having only one damper at location 12. It is indeed the location that could have been thought to be the most frequently used in all cases as it is common to see dampers located at the top of buildings, although it appeared that the privileged position for this 2D-structure was in fact location 11. For $c=5$, the damping ratios achieved are given underneath and show that: the values increase with the modes, mode 1 has nearly no damping, and that there is a huge increase between mode 1 and 2 and again between mode 2 and mode 3, with $\xi_3 \approx 2\xi_4$.



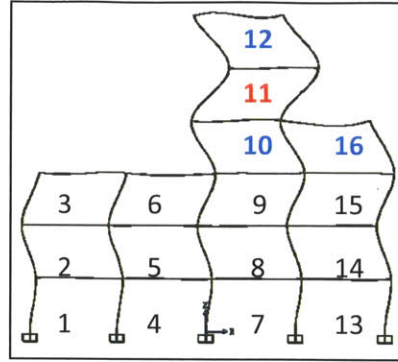
mode	ξ_m
1	1,4%
2	20,3%
3	40,1%
4	44,6%
5	48,3%
6	51,6%
7	0,1%
8	0,3%
9	0,0%
10	0,0%
11	0,0%
12	0,0%

Figures 90: the shape of mode 5 and the results of the optimization process for $c = 5, \xi_{5|target} = 10\% - 20\%$

When given a constraint on the first five modes, the results are exactly the same as in previous case studies.

6. Damping ratio targets for modes 1, 2, 3, 4, 5 and 6

For mode 6 alone it appears that the most efficient locations are, in order of importance: 11, 12, then 10 and 16. Obviously these locations are on the asymmetrical top part of the structure as it seems to be at the top that the drift ratio is the most important.



Figures 91: the shape of mode 6

When given a constraint on the first five modes, the results are once again exactly the same as in previous case studies.

7. Damping ratio targets for mode 12

Although this is a damping ratio that does not have to be taken into account with regards to the other first six modes which are more important, it is the first horizontal mode after the vertical ones 7 to 11. The most important locations are located on the first floor and the third floor. For $c = 3$, $\xi_{12|target} = 10\%$ mode 1 is more than 15% damped, mode 2 is more than 12% damped and mode 3 is more than 56% damped. This shows that if mode 12 really needs to be damped, a constraint can be targeted on this mode only and the first modes will have nonetheless efficient damping. However, in nearly all previous case studies it appeared that mode 12 was never efficiently damped, apart from the case $c = 2.3$, $\xi_{12|target} = 30\%$. Although it was interesting to see how the first horizontal mode of the secondary modes behaved, it is not of influence in the general behavior of the building and has a very low participation factor.

8. Conclusion

The most important conclusion is that the general behavior of the damping ratios is to increase with the modes. As this increase is significant, it appeared that by giving a constraint on the targeted damping ratios of the first two modes all the other first modes were damped enough. More precise relations between some damping ratios were found, but as it is only a 2D-structure they should be verified on a real structure before generalizing these relations. Lastly, it would be interesting to see if in a real structure the damping ratio of the third mode has to be targeted or if it is unnecessary as in this example.

H. 2D- Example: non-uniform prices

The optimization process described earlier is very rich and can take into account many parameters. The first part of the 2D-example studied previously corresponds to the easiest optimization problem: a single type of damper used, prices and damping constants being constant for all locations. This led us to find general relations between modes and damping ratios. The second part of the study of this 2D-example will now focus on the influence of variable prices on the results obtained in the first part. The damping constants are kept constant and equal throughout the structure.

The optimization problem can now be formulated as:

- $J=1, K=16, M=12$
- Determine the vector $\alpha = (\alpha_k)_{k \in [1, K]}$ that minimizes the cost of the installation of dampers:

$$Cost = \sum_k p_k \alpha_k = P^T \alpha.$$

- Knowing that the constraints are:
$$\begin{cases} c \cdot \sum_k x_{km} \alpha_k \geq \xi_{m|target} \\ \alpha_k \in \{0,1\}, \forall k \in [1, K] \end{cases}$$

Three different prices will be considered in this case study. The most expensive locations are on top of the building. An explanation for this could be that adding dampers add mass at the top, which will induce an increase of material throughout the building to counterbalance this and therefore an increase in price. The second most expensive locations are the ones on the sides, which can be considered as equivalent to the façade at eye-level of a 3D-structure. In real life this increase in prices for façades is justified by the fact that architects rarely appreciate these devices as artistic decorations. Lastly, the cheapest dampers are found in the middle of the building, where it does not really influence the architectural or structural design.

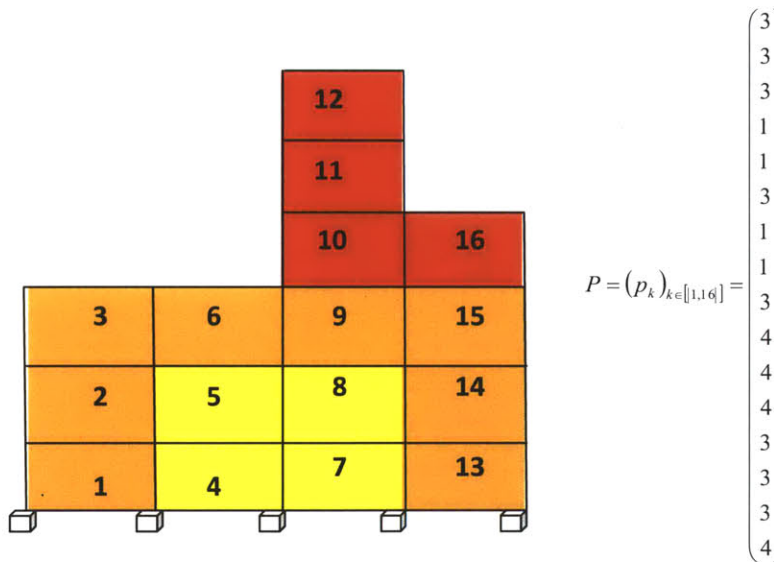


Figure 92: Distribution of the prices throughout the structure. Red represents the most expensive locations, followed by orange and yellow being the cheapest ones.

The study of the impact of the vector P on the optimization process will be shown by recalculating some cases studied in the first part of this example.

1. Damping ratio targeted only for mode 1

The most efficient locations to damp mode 1 were previously found to be, by order of importance: the 2nd floor (2, 5, 8, 14), then the 4th floor (10, 16) and then the 3rd floor (3, 6, 9, 15). It is interesting to see how cases studied earlier for $\xi_{1|target} = 20\% - 30\%$ are modified when P is no longer equal to 1.

$\xi_{1|t \text{ arg et}} = 20\%$
 $c = 2$

location/mode	Before Cost=31		After Cost=25	
	$\alpha_{ opt}$	ξ_m	$\alpha_{ opt}$	ξ_m
1	0	20,4%	0	20,1%
2	1	31,8%	1	15,2%
3	1	48,6%	1	42,8%
4	0	61,8%	1	53,6%
5	1	75,2%	1	68,5%
6	1	76,0%	1	44,7%
7	0	0,0%	1	0,0%
8	1	0,0%	1	0,0%
9	1	0,0%	1	0,0%
10	1	0,0%	0	0,0%
11	1	0,1%	0	0,1%
12	0	4,0%	0	4,9%
13	0		0	
14	1		1	
15	1		1	
16	1		1	

$\xi_{1|t \text{ arg et}} = 30\%$
 $c = 5$

location/mode	Before Cost=15		After Cost=10	
	$\alpha_{ opt}$	ξ_m	$\alpha_{ opt}$	ξ_m
1	0	31,6%	0	30,6%
2	1	40,7%	1	24,8%
3	0	27,3%	0	19,4%
4	0	115,1%	1	56,2%
5	1	102,3%	1	114,5%
6	0	82,1%	0	37,8%
7	0	0,0%	1	0,0%
8	1	0,0%	1	0,0%
9	0	0,0%	0	0,0%
10	1	0,0%	0	0,0%
11	0	0,0%	0	0,0%
12	0	0,7%	0	2,7%
13	0		0	
14	1		1	
15	0		0	
16	1		0	

Figures 93 and 94: cases 1 and 2. Comparison between the optimization process when $P=1$ (before) and when P varies (after). In blue: the locations that have a damper in both cases; in yellow, those that differ

We can see on figure 93 that the most expensive locations, 10/11 and 10/16, are replaced in both cases by the locations 4 and 7. This change tends to decrease the resulting damping ratios of modes 1 to 6, mode 2 being the most affected with a damping ratio that is nearly divided by two. These changes however reduce greatly the overall cost by 19,4% and 33,3% respectively. This means that by keeping the same amount of dampers, but moving two of them from efficient locations to low-efficient locations is enough to reduce the costs significantly while achieving the targeted damping. Although the principle of replacing efficient and expensive dampers by the same number of cheap and yet inefficient dampers seems very attractive, it does not work so easily in general. If we indeed look at the example underneath, we see that one damper installed in a non-efficient location (14) had to be replaced by two dampers (also in non-efficient but cheaper locations), resulting in a reduction of cost of only 12,5%. It might still be worthy as the damping ratios increase from “before” to “after”, but if the given constraints are considered to be already a top boundary of what has to be achieved, then this change of solution does not seem as impressive as the one seen right before.

$\xi_{1|target} = 20\%$
 $c = 5$

location/mode	Before Cost=8		After Cost=7	
	α_{opt}	ξ_m	α_{opt}	ξ_m
1	0	23,2%	0	24,8%
2	1	14,5%	1	21,1%
3	0	0,3%	0	19,3%
4	0	37,4%	1	46,8%
5	1	102,3%	1	89,1%
6	0	34,7%	0	29,2%
7	0	0,0%	1	0,0%
8	1	0,0%	1	0,0%
9	0	0,0%	0	0,0%
10	0	0,0%	0	0,0%
11	0	0,0%	0	0,0%
12	0	0,5%	0	2,5%
13	0		0	
14	1		0	
15	0		0	
16	0		0	

Figures 95: case 3. Same constraint as in case 1 but with a larger c.

However, there is an important difference of cost between cases 1 and 3: 25 to 7, which represents - 72%. This change is only due to the fact that c was increased from 2 to 5. In order not to complicate the optimization problem too quickly, c was taken as a constant that is not optimized in this 2D-example, but this result still highlights two things: how by adding a few variables an optimization problem can become very complicated, and how much a little change in variables can be significant on the results.

2. Damping ratio targeted only for mode 2

This is another example of the fact that some optimizations are not giving impressive results because there is not much to do to improve the existing solution. The most efficient locations for damping mode 2 were, by order of importance: 11, then 12, then the 4th floor. By changing the prices in this case one damper from a non-efficient location has to be replaced by two dampers, also from non-efficient locations but cheaper. The reduction of cost is only of 5,0% and there is not even a remarkable increase

in damping: the most important modes are the first three and although ξ_1 increases by 32,7%, it remains around 5% and does not reach the 10% stage.

$\xi_{2|target} = 20\%$
 $c = 1$

location/mode	Before Cost=20		After Cost=19	
	α_{opt}	ξ_m	α_{opt}	ξ_m
1	1	4,9%	0	6,5%
2	0	20,1%	0	20,5%
3	0	23,2%	0	21,3%
4	1	30,1%	1	32,0%
5	0	19,1%	1	28,2%
6	0	32,2%	0	35,4%
7	1	0,0%	1	0,0%
8	0	0,1%	1	0,1%
9	0	0,0%	0	0,0%
10	1	0,0%	1	0,0%
11	1	0,0%	1	0,0%
12	1	1,2%	1	0,5%
13	0		0	
14	0		0	
15	0		0	
16	1		1	

Figure 96: case 4

3. Damping ratio targeted for modes 1 and 2

As seen in the first part of this 2D-example, by targeting the first two modes the whole structure is enough damped. Therefore the second part of the study of this 2D-example will be ended by the study of the impact of P on the optimization process by looking at what happens when $\xi_{1|target} = \xi_{2|target} = 20\%$.

$\xi_{1|t} = \xi_{2|t} = 20\%$
 $c = 3$

location/mode	Before Cost=18		After Cost=13	
	α_{opt}	ξ_m	α_{opt}	ξ_m
1	0	21,4%	0	20,8%
2	1	24,5%	1	22,6%
3	0	27,7%	0	19,7%
4	0	74,6%	1	56,9%
5	1	69,8%	1	68,7%
6	0	56,5%	0	36,9%
7	0	0,0%	1	0,0%
8	1	0,0%	1	0,0%
9	0	0,0%	0	0,0%
10	1	0,0%	0	0,0%
11	0	0,0%	0	0,0%
12	0	2,6%	0	1,7%
13	0		0	
14	1		1	
15	1		0	
16	1		1	

$\xi_{1|t} = \xi_{2|t} = 20\%$
 $c = 10$

location/mode	Before Cost=8		After Cost=6	
	α_{opt}	ξ_m	α_{opt}	ξ_m
1	0	31,0%	0	31,0%
2	1	91,7%	0	91,8%
3	0	40,8%	0	40,8%
4	0	37,3%	0	37,7%
5	1	160,6%	1	161,0%
6	0	149,9%	0	149,8%
7	0	0,0%	0	0,0%
8	0	0,0%	1	0,0%
9	0	0,0%	0	0,0%
10	0	0,0%	0	0,0%
11	1	0,0%	1	0,0%
12	0	0,5%	0	0,2%
13	0		0	
14	0		0	
15	0		0	
16	0		0	

Figures 97 and 98: cases 5 and 6

When modes 1 and 2 were coupled, the most important locations were the ones on the 2nd floor (2, 5, 8 and 14) and n°11. For case 4 (c=3) costs can be reduced by nearly 30% by exchanging locations of two dampers while keeping equivalent results.

Finally, the last case, although not very realistic with such damping ratios, shows that for a certain value of c dampers on the same (regular) floor are equivalent. We could also note that tripling c leads to use half as much dampers and reduce the cost by half too, but reality would be far different as the price would be also a function of c so it is unlikely that the cost be reduced by half.

4. Conclusion

A few comments have to be made on the second part of the 2D-example. First, the plan of locations of dampers is globally similar to when P was not a variable, although one or two dampers are changed location to reduce the costs. This leads to the second remark which is that by processing to an optimization the costs can be greatly reduced, even by a third, and therefore shows the use of creating an optimization process instead of simply locating dampers with regards to the geometry of the modes.

CONCLUSION

The primary goal of this thesis was to optimize the installation of dampers in a building. The optimization problem, defined in Part II, considers a building's geometry, mode shapes, types of dampers that may be used and prices associated with each location and type of damper. Because linear optimization problems are easier and faster to solve, optimal elongations for each type of damper and its associated location should be a linear function of the perturbation. Part I therefore focused on four common damper configurations by: solving for the exact elongations and then assessing the responses of vertical and horizontal loads to determine whether linear relationships could be found between elongations and perturbations. Part I concluded that these types of relationships could be found in most cases and the design of the configurations was optimized in addition. Results of Part I could be used for the optimization problem if these four types of dampers were possibly installed in a building.

Part II analyzed a 2-Dimensional example, along with results from Part I, to better illustrate the way installation of dampers could be optimized. The 2D structure was assumed tall enough to be sensitive to earthquakes while also remaining asymmetrical in order to complicate the optimization problem. Additionally, the 2D structure was small enough for hand calculations that served to check the results of the optimization function. The first part of this example was designed to study damping ratios and proved that if constraints were put on damping ratios of the first two mode shapes than the other modes of the structure would be damped enough in the event of an earthquake. It would be interesting to see if this conclusion has to be generalized to the first three modes for a real structure. Because the first part of the example served to optimize the locations of dampers (one type of dampers with the same properties for all locations), the second part of the example was designed to analyze how results would change after adding a new variable and three different prices were set for the different locations. After running the same optimization as in the first part of the example, it could be recognized that the location of several dampers needed to be changed, despite a similar general positioning scheme. After understanding how to damp the first two (three) modes efficiently, one can predict the general positioning scheme, though with slight variations to reduce the overall damping costs. Additionally, it must be noted that costs between an optimized solution and a non-optimized solution could vary significantly. Although the optimization process was carried out with few variables in the 2D-example,

many more constraints and variables can be taken into account, as demonstrated in the general optimization problem description in Part II.

In conclusion, the general optimization problem analyzed in this thesis functions adequately and provided useful values from the study of the four common configurations. Future studies of the optimization problem should be carried out on a real building using the types of dampers discussed.

APPENDIXES

I- Appendix 1: details of the calculations of the elongation of dampers in configuration 2

In order to calculate the displacement of E, both members AE and ED are assumed to be rigid and therefore with constant length.

$$\begin{aligned}
 l_{AE_{initial}} &= l_{AE_{final}} \\
 \Rightarrow \sqrt{(x_A + u_A - x_E - u_E)^2 + (y_A + v_A - y_E - v_E)^2} &= \sqrt{(x_A - x_E)^2 + (y_A - y_E)^2} \\
 \Rightarrow 2(x_A - x_E)(u_A - u_E) + (u_A - u_E)^2 + 2(y_A - y_E)(v_A - v_E) + (v_A - v_E)^2 &= 0 \\
 \Rightarrow u_E^2 + 2u_E(x_E - x_A - u_A) + v_E^2 + 2v_E(y_E - y_A - v_A) + u_A(u_A + 2x_A - 2x_E) + v_A(v_A + 2y_A - 2y_E) &= 0 \\
 \Rightarrow u_E^2 + 2u_E\alpha + v_E^2 + 2v_E\beta + u_A\gamma + v_A\delta &= 0
 \end{aligned}$$

$$\begin{aligned}
 l_{ED_{initial}} &= l_{ED_{final}} \\
 \Rightarrow u_E^2 + 2u_E(x_E - x_D - u_D) + v_E^2 + 2v_E(y_E - y_D - v_D) + u_D(u_D + 2x_D - 2x_E) + v_D(v_D + 2y_D - 2y_E) &= 0
 \end{aligned}$$

These two equations then lead us to a system of two equations for two unknowns. The only problem is that they are quadratic equations and not linear ones. To simplify these equations for display purposes, new variables, functions of the known coordinates, are introduced.

$$\begin{cases}
 u_E^2 + 2u_E(x_E - x_A - u_A) + v_E^2 + 2v_E(y_E - y_A - v_A) + u_A(u_A + 2x_A - 2x_E) + v_A(v_A + 2y_A - 2y_E) = 0 \\
 u_E^2 + 2u_E(x_E - x_D - u_D) + v_E^2 + 2v_E(y_E - y_D - v_D) + u_D(u_D + 2x_D - 2x_E) + v_D(v_D + 2y_D - 2y_E) = 0
 \end{cases}$$

$$\Rightarrow \begin{cases}
 u_E^2 + 2u_E\alpha + v_E^2 + 2v_E\beta + u_A\gamma + v_A\delta = 0 \\
 2u_E(x_D + u_D - x_A - u_A) + 2v_E(y_D + v_D - y_A - v_A) + u_A(u_A + 2x_A - 2x_E) + v_A(v_A + 2y_A - 2y_E) - u_D(u_D + 2x_D - 2x_E) - v_D(v_D + 2y_D - 2y_E) = 0
 \end{cases}$$

$$\Rightarrow \begin{cases}
 u_E^2 + 2u_E\alpha + v_E^2 + 2v_E\beta + u_A\gamma + v_A\delta = 0 \\
 2u_E\varepsilon + 2v_E\eta + u_A\gamma + v_A\delta - u_D\lambda - v_D\mu = 0
 \end{cases}$$

The resulting system is expressed with a quadratic equation for v_e and a linear expression for u_e depending on v_e .

$$\Rightarrow \begin{cases} u_E^2 + 2u_E\alpha + v_E^2 + 2v_E\beta + u_A\gamma + v_A\delta = 0 \\ u_E = -v_E \frac{\eta}{\varepsilon} - u_A \frac{\gamma}{2\varepsilon} - v_A \frac{\delta}{2\varepsilon} + u_D \frac{\lambda}{2\varepsilon} + v_D \frac{\mu}{2\varepsilon} \end{cases}$$

$$\Rightarrow \begin{cases} u_E = -v_E\xi + \varphi \\ v_E^2(1 + \xi^2) + 2v_E(\beta - \varphi\xi - \alpha\xi) + \varphi^2 + 2\alpha\varphi + u_A\gamma + v_A\delta = 0 \end{cases}$$

By using Maple the system is expressed with the coordinates of the nodes instead of using the substitution unknowns.

Definition of the system to find both unknowns u_e and v_e

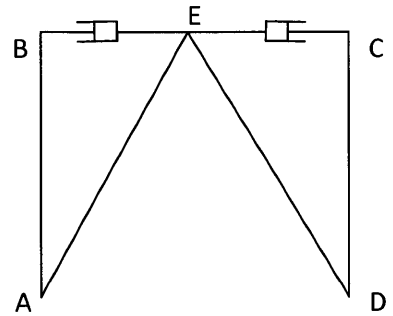
$$\begin{aligned} &> eq_{ue} := -v_e \cdot \xi + \varphi; \\ &eq_{ue} := -\frac{v_e(y_d + v_d - y_a - v_a)}{x_d + u_d - x_a - u_a} + \frac{1}{2} \frac{u_d(u_d - 2x_e + 2x_d) + v_d(v_d - 2y_e + 2y_d) - u_a(u_a - 2x_e + 2x_a) - v_a(v_a - 2y_e + 2y_a)}{x_d + u_d - x_a - u_a} \\ &> eq_{ve} := (1 + \xi^2) \cdot v_e^2 + 2 \cdot v_e \cdot (\beta - \varphi \xi - \alpha \xi) + \varphi^2 + 2 \cdot \alpha \cdot \varphi + u_a \cdot \text{gamma} + v_a \cdot \delta; \\ eq_{ve} := &\left(1 + \frac{(y_d + v_d - y_a - v_a)^2}{(x_d + u_d - x_a - u_a)^2} \right) v_e^2 + 2 v_e \left(y_e - y_a - v_a \right. \\ &- \frac{1}{2} \frac{(u_d(u_d - 2x_e + 2x_d) + v_d(v_d - 2y_e + 2y_d) - u_a(u_a - 2x_e + 2x_a) - v_a(v_a - 2y_e + 2y_a)) (y_d + v_d - y_a - v_a)}{(x_d + u_d - x_a - u_a)^2} \\ &- \left. \frac{(x_e - x_a - u_a) (y_d + v_d - y_a - v_a)}{x_d + u_d - x_a - u_a} \right) \\ &+ \frac{1}{4} \frac{(u_d(u_d - 2x_e + 2x_d) + v_d(v_d - 2y_e + 2y_d) - u_a(u_a - 2x_e + 2x_a) - v_a(v_a - 2y_e + 2y_a))^2}{(x_d + u_d - x_a - u_a)^2} \\ &+ \frac{(x_e - x_a - u_a) (u_d(u_d - 2x_e + 2x_d) + v_d(v_d - 2y_e + 2y_d) - u_a(u_a - 2x_e + 2x_a) - v_a(v_a - 2y_e + 2y_a))}{x_d + u_d - x_a - u_a} + u_a(u_a - 2x_e \\ &+ 2x_a) + v_a(v_a - 2y_e + 2y_a) \end{aligned}$$

II- Appendix 2: exact expression of the elongation of dampers in configuration 2

As the expressions of the elongation was too long to be given in this document (38 pages only for the elongation of damper 1), a few assumptions were made to reduce it to a smaller expression.

Assumptions:

- A is taken as the origin of the frame: $x_a = y_a = 0$
- The frame is rectangular
- E is in its optimal location, on the middle of the member BC



With these assumptions, the expression was still too long to be copied in this appendix, so another assumption had to be made.

As dampers are usually to control the response of a building to seismic loads, so horizontal loads, elongations were calculated as if there were no vertical displacements.

It was seen earlier that there were many possible mathematical solutions, but only one physical solution. Both formulas for the total elongation are given underneath. For memory, the total elongation is the sum of both contributions of dampers for a given frame: $e_{total} = e_{km} = \sqrt{e_1^2 + e_2^2}$. It has no physical signification but is the equivalent elongation used to calculate the damping ratios.

With the same approximations, apart from E which does not have any constraint, the expression of the elongation of the damper in configuration 3 is 17 pages long, and 47 pages long for configuration 4. This is the reason why this appendix only contains the expressions for dampers in configuration 2.

1st solution for the total elongation:

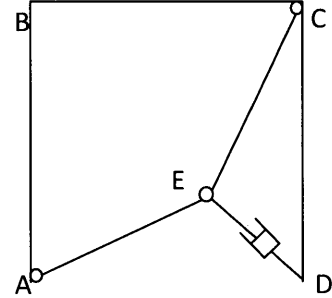
$$\begin{aligned}
 &> \text{tot}_1 := \text{sqrt}((\text{elongation}_{d1-1})^2 + (\text{elongation}_{d2-1})^2); \\
 &\text{tot}_1 := \\
 &\left(\left(\frac{1}{2} \left(4u_b^2 - 4u_b x_c - \frac{4u_b(u_d(u_d+x_c) - u_a(u_a-x_c))}{x_c + u_d - u_a} + x_c^2 + \frac{2x_c(u_d(u_d+x_c) - u_a(u_a-x_c))}{x_c + u_d - u_a} \right. \right. \right. \\
 &\quad \left. \left. \left. + \frac{(u_d(u_d+x_c) - u_a(u_a-x_c))^2}{(x_c + u_d - u_a)^2} + 4 \left(-y_b + v_d + \frac{1}{2} \sqrt{4y_b^2 - u_a^2 + 2u_a x_c + 2u_d u_a - 2u_d x_c - u_d^2} \right)^2 - \frac{1}{2} \sqrt{x_c^2} \right)^2 \right. \right. \\
 &\quad \left. \left. + \left(\frac{1}{2} \left(x_c^2 + 4x_c u_c - \frac{2x_c(u_d(u_d+x_c) - u_a(u_a-x_c))}{x_c + u_d - u_a} + 4u_c^2 - \frac{4u_c(u_d(u_d+x_c) - u_a(u_a-x_c))}{x_c + u_d - u_a} \right. \right. \right. \right. \\
 &\quad \left. \left. \left. + \frac{(u_d(u_d+x_c) - u_a(u_a-x_c))^2}{(x_c + u_d - u_a)^2} + 4y_c^2 + 8y_c v_c - 8y_c y_b - 8y_c \left(-y_b + v_d + \frac{1}{2} \sqrt{4y_b^2 - u_a^2 + 2u_a x_c + 2u_d u_a - 2u_d x_c - u_d^2} \right) \right. \right. \right. \\
 &\quad \left. \left. \left. + 4v_c^2 - 8v_c y_b - 8v_c \left(-y_b + v_d + \frac{1}{2} \sqrt{4y_b^2 - u_a^2 + 2u_a x_c + 2u_d u_a - 2u_d x_c - u_d^2} \right) + 4y_b^2 + 8y_b \left(-y_b + v_d \right. \right. \right. \right. \\
 &\quad \left. \left. \left. + \frac{1}{2} \sqrt{4y_b^2 - u_a^2 + 2u_a x_c + 2u_d u_a - 2u_d x_c - u_d^2} \right) + 4 \left(-y_b + v_d + \frac{1}{2} \sqrt{4y_b^2 - u_a^2 + 2u_a x_c + 2u_d u_a - 2u_d x_c - u_d^2} \right)^2 \right)^2 \right. \\
 &\quad \left. \left. - \frac{1}{2} \sqrt{x_c^2 + 4y_c^2 - 8y_c y_b + 4y_b^2} \right)^2 \right)^{1/2}
 \end{aligned}$$

2nd solution for the total elongation:

$$\begin{aligned}
 &> \text{tot}_2 := \text{sqrt}((\text{elongation}_{d1-2})^2 + (\text{elongation}_{d2-2})^2); \\
 &\text{tot}_2 := \\
 &\left(\left(\frac{1}{2} \left(4u_b^2 - 4u_b x_c - \frac{4u_b(u_d(u_d+x_c) - u_a(u_a-x_c))}{x_c + u_d - u_a} + x_c^2 + \frac{2x_c(u_d(u_d+x_c) - u_a(u_a-x_c))}{x_c + u_d - u_a} \right. \right. \right. \\
 &\quad \left. \left. \left. + \frac{(u_d(u_d+x_c) - u_a(u_a-x_c))^2}{(x_c + u_d - u_a)^2} + 4 \left(-y_b + v_d - \frac{1}{2} \sqrt{4y_b^2 - u_a^2 + 2u_a x_c + 2u_d u_a - 2u_d x_c - u_d^2} \right)^2 - \frac{1}{2} \sqrt{x_c^2} \right)^2 \right. \right. \\
 &\quad \left. \left. + \left(\frac{1}{2} \left(x_c^2 + 4x_c u_c - \frac{2x_c(u_d(u_d+x_c) - u_a(u_a-x_c))}{x_c + u_d - u_a} + 4u_c^2 - \frac{4u_c(u_d(u_d+x_c) - u_a(u_a-x_c))}{x_c + u_d - u_a} \right. \right. \right. \right. \\
 &\quad \left. \left. \left. + \frac{(u_d(u_d+x_c) - u_a(u_a-x_c))^2}{(x_c + u_d - u_a)^2} + 4y_c^2 + 8y_c v_c - 8y_c y_b - 8y_c \left(-y_b + v_d - \frac{1}{2} \sqrt{4y_b^2 - u_a^2 + 2u_a x_c + 2u_d u_a - 2u_d x_c - u_d^2} \right) \right. \right. \right. \\
 &\quad \left. \left. \left. + 4v_c^2 - 8v_c y_b - 8v_c \left(-y_b + v_d - \frac{1}{2} \sqrt{4y_b^2 - u_a^2 + 2u_a x_c + 2u_d u_a - 2u_d x_c - u_d^2} \right) + 4y_b^2 + 8y_b \left(-y_b + v_d \right. \right. \right. \right. \\
 &\quad \left. \left. \left. - \frac{1}{2} \sqrt{4y_b^2 - u_a^2 + 2u_a x_c + 2u_d u_a - 2u_d x_c - u_d^2} \right) + 4 \left(-y_b + v_d - \frac{1}{2} \sqrt{4y_b^2 - u_a^2 + 2u_a x_c + 2u_d u_a - 2u_d x_c - u_d^2} \right)^2 \right)^2 \right. \\
 &\quad \left. \left. - \frac{1}{2} \sqrt{x_c^2 + 4y_c^2 - 8y_c y_b + 4y_b^2} \right)^2 \right)^{1/2}
 \end{aligned}$$

III- Appendix 3: details of the calculations of the elongation of dampers in configuration

The elongation of the damper in the toggle system is calculated in a similar way as the elongations were calculated for the configuration 2. The unknowns u_e and v_e are found by expressing the fact that the elements AE and EC are rigid and cannot elongate.



$$l_{AE_{initial}} = l_{AE_{final}}$$

$$\Rightarrow u_E^2 + 2u_E(x_E - x_A - u_A) + v_E^2 + 2v_E(y_E - y_A - v_A) + u_A(u_A + 2x_A - 2x_E) + v_A(v_A + 2y_A - 2y_E) = 0$$

$$\Rightarrow u_E^2 + 2u_E\alpha + v_E^2 + 2v_E\beta + u_A\gamma + v_A\delta = 0$$

$$l_{EC_{initial}} = l_{EC_{final}}$$

$$\Rightarrow 2(x_C - x_E)(u_C - u_E) + (u_C - u_E)^2 + 2(y_C - y_E)(v_C - v_E) + (v_C - v_E)^2$$

$$\Rightarrow u_E^2 + 2u_E(x_E - x_C - u_C) + v_E^2 + 2v_E(y_E - y_C - v_C) + u_C(u_C + 2x_C - 2x_E) + v_C(v_C + 2y_C - 2y_E) = 0$$

A similar system as seen previously is obtained.

$$\Rightarrow \begin{cases} u_E^2 + 2u_E\alpha + v_E^2 + 2v_E\beta + u_A\gamma + v_A\delta = 0 \\ 2u_E\varepsilon + 2v_E\eta + u_A\gamma + v_A\delta - u_C\lambda - v_C\mu = 0 \end{cases}$$

$$\Rightarrow \begin{cases} u_E^2 + 2u_E\alpha + v_E^2 + 2v_E\beta + u_A\gamma + v_A\delta = 0 \\ u_E = -v_E \frac{\eta}{\varepsilon} - u_A \frac{\gamma}{2\varepsilon} - v_A \frac{\delta}{2\varepsilon} + u_C \frac{\lambda}{2\varepsilon} + v_C \frac{\mu}{2\varepsilon} \end{cases}$$

$$\Rightarrow \begin{cases} u_E = -v_E\xi + \varphi \\ v_E^2(1 + \xi^2) + 2v_E(\beta - \varphi\xi - \alpha\xi) + \varphi^2 + 2\alpha\varphi + u_A\gamma + v_A\delta = 0 \end{cases}$$

Once we have solved for u_e and v_e , the elongation can be calculated.

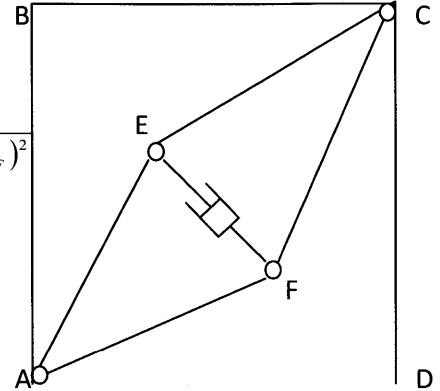
IV- Appendix 4: details of the calculations of the elongation of dampers in configuration 4

The steps and the equations are similar to both previous cases, but with four unknowns instead of two: u_e , v_e and u_f , v_f .

The elongation is given by:

$$e = \sqrt{(x_E + u_E - x_F - u_F)^2 + (y_E + v_E - y_F - v_F)^2} - \sqrt{(x_E - x_F)^2 + (y_E - y_F)^2}$$

The method to find the unknowns u_e and v_e is the same as before and uses the assumption that both members AE and EC are rigid and cannot elongate.



$$l_{AE_{initial}} = l_{AE_{final}}$$

$$\Rightarrow u_E^2 + 2u_E(x_E - x_A - u_A) + v_E^2 + 2v_E(y_E - y_A - v_A) + u_A(u_A + 2x_A - 2x_E) + v_A(v_A + 2y_A - 2y_E) = 0$$

$$\Rightarrow u_E^2 + 2u_E\alpha + v_E^2 + 2v_E\beta + u_A\gamma + v_A\delta = 0$$

$$l_{EC_{initial}} = l_{EC_{final}}$$

$$\Rightarrow 2(x_C - x_E)(u_C - u_E) + (u_C - u_E)^2 + 2(y_C - y_E)(v_C - v_E) + (v_C - v_E)^2 = 0$$

$$\Rightarrow u_E^2 + 2u_E(x_E - x_C - u_C) + v_E^2 + 2v_E(y_E - y_C - v_C) + u_C(u_C + 2x_C - 2x_E) + v_C(v_C + 2y_C - 2y_E) = 0$$

$$\Rightarrow \begin{cases} u_E^2 + 2u_E\alpha + v_E^2 + 2v_E\beta + u_A\gamma + v_A\delta = 0 \\ u_E = -v_E \frac{\eta}{\varepsilon} - u_A \frac{\gamma}{2\varepsilon} - v_A \frac{\delta}{2\varepsilon} + u_D \frac{\lambda}{2\varepsilon} + v_D \frac{\mu}{2\varepsilon} \end{cases}$$

$$\Rightarrow \begin{cases} u_E = -v_E\xi + \varphi \\ v_E^2(1 + \xi^2) + 2v_E(\beta - \varphi\xi - \alpha\xi) + \varphi^2 + 2\alpha\varphi + u_A\gamma + v_A\delta = 0 \end{cases}$$

We have the exact same set of equations for the unknowns u_f and v_f :

$$\begin{aligned}
l_{AF_{initial}} &= l_{AF_{final}} \\
\Rightarrow u_F^2 + 2u_F(x_F - x_A - u_A) + v_F^2 + 2v_F(y_F - y_A - v_A) + u_A(u_A + 2x_A - 2x_F) + v_A(v_A + 2y_A - 2y_F) &= 0 \\
\Rightarrow u_F^2 + 2u_F\alpha + v_F^2 + 2v_F\beta + u_A\gamma + v_A\delta &= 0 \\
l_{FC_{initial}} &= l_{FC_{final}} \\
\Rightarrow 2(x_C - x_F)(u_C - u_F) + (u_C - u_F)^2 + 2(y_C - y_F)(v_C - v_F) + (v_C - v_F)^2 \\
\Rightarrow u_F^2 + 2u_F(x_F - x_C - u_C) + v_F^2 + 2v_F(y_F - y_C - v_C) + u_C(u_C + 2x_C - 2x_F) + v_C(v_C + 2y_C - 2y_F) &= 0 \\
\Rightarrow \begin{cases} u_E = -v_E\xi + \varphi \\ v_E^2(1 + \xi^2) + 2v_E(\beta - \varphi\xi - \alpha\xi) + \varphi^2 + 2\alpha\varphi + u_A\gamma + v_A\delta = 0 \end{cases}
\end{aligned}$$

The only thing that changes is the definition of the substituted symbols for each damper:

$$\begin{array}{lll}
\alpha_1 := x_e - x_a - u_a : & \alpha_2 := x_f - x_a - u_a : & \varepsilon := x_c + u_c - x_a - u_a : \\
\beta_1 := y_e - y_a - v_a : & \beta_2 := y_f - y_a - v_a : & \eta := y_c + v_c - y_a - v_a : \\
\text{gammaa}_1 := u_a - 2 \cdot x_e + 2 \cdot x_a & \text{gammaa}_2 := u_a - 2 \cdot x_f + 2 \cdot x_a : & \xi := \frac{\eta}{\varepsilon} ; \\
\delta_1 := v_a - 2 \cdot y_e + 2 \cdot y_a : & \delta_2 := v_a - 2 \cdot y_f + 2 \cdot y_a : & \phi_1 := \frac{u_c \cdot \lambda_1 + v_c \cdot \mu_1 - u_a \cdot \text{gammaa}_1 - v_a \cdot \delta_1}{2 \cdot \varepsilon} ; \\
\lambda_1 := u_c - 2 \cdot x_e + 2 \cdot x_c : & \lambda_2 := u_c - 2 \cdot x_f + 2 \cdot x_c : & \phi_2 := \frac{u_c \cdot \lambda_2 + v_c \cdot \mu_2 - u_a \cdot \text{gammaa}_2 - v_a \cdot \delta_2}{2 \cdot \varepsilon} ; \\
\mu_1 := v_c - 2 \cdot y_e + 2 \cdot y_c : & \mu_2 := v_c - 2 \cdot y_f + 2 \cdot y_c : &
\end{array}$$

V- Appendix 5: Results of the study of the 2D-structure

As explained earlier, the 2D-structure was modeled on SAP, and the results of the displacement of the nodes for each mode were then used to run the optimization in Maple. For each case study the vector $\xi_{m|target}$ had to be first set. The range of c was then defined so that the structure would evolve from having only one damper to having nearly all locations occupied by dampers. As mentioned earlier, the optimization function used returns a vector $\alpha = (\alpha_k)_{k \in [1, K]}$ such that $\alpha_k \in [0, 1]$. This vector was then translated to the vector $\alpha_{|opt}$ which has only binary variables. The damping ratios achieved were then calculated using $\alpha_{|opt}$. Although the tables of results in Appendix 5 only contain $\alpha_{|opt}$ and ξ_m , α was checked to see if there was only one damper such that $\alpha_k \in]0, 1[$ or several ones. Usually there was only one, and by increasing c , this damper in position k would be the one no longer necessary, but when there were two dampers such that $\alpha_{k1} \in]0, 1[, \alpha_{k2} \in]0, 1[$ then the interpretation was not as straight forward.

On each table there are two columns: $\alpha_{|opt}$ and ξ_m . Therefore, the numbers 1 to 12 either refer to the location of the damper (1 to 16 for $\alpha_{|opt}$) or to the mode (1 to 12 for ξ_m).

Case study 1: $\xi_{m|target}$ has one non-zero value, $\xi_{1|target}$

❖ $\xi_{1|target} = 5\%$

location /mode	case 1: c=0.4		case 2: c=0.5		case 3: c=0.6		case 4: c=0.7		case 5: c=0.8		case 6: c=0.9	
	α_{opt}	ξ_m	α_{opt}	ξ_m	α_{opt}	ξ_m	α_{opt}	ξ_m	α_{opt}	ξ_m	α_{opt}	ξ_m
1	1	5,3%	0	5,1%	0	5,2%	0	5,54%	0	5,1%	0	
2	1	8,0%	1	8,0%	1	9,5%	1	5,72%	1	6,5%	1	
3	1	12,8%	1	12,2%	0	10,2%	0	9,08%	0	4,4%	0	
4	1	15,4%	0	15,4%	0	16,1%	0	18,75%	0	18,4%	0	
5	1	17,0%	1	18,8%	1	19,2%	1	18,29%	1	16,4%	1	
6	1	15,7%	1	19,0%	0	19,7%	0	14,91%	0	13,1%	0	
7	1	0,0%	0	0,0%	0	0,0%	0	0,00%	0	0,0%	0	
8	1	0,0%	1	0,0%	1	0,0%	1	0,00%	1	0,0%	1	
9	1	0,0%	1	0,0%	1	0,0%	1	0,00%	0	0,0%	0	
10	1	0,0%	1	0,0%	1	0,0%	1	0,00%	1	0,0%	1	
11	1	0,0%	1	0,0%	1	0,0%	0	0,01%	0	0,0%	0	
12	0	1,5%	0	1,0%	0	0,7%	0	0,78%	0	0,1%	0	
13	1		0		0		0		0		0	
14	1		1		1		1		1		1	
15	1		1		1		1		0		0	
16	1		1		1		1		1		1	

location /mode	case 7: c=1		case 8: c=1.25		case 9: c=1.5		case 10: c=2.0		case 11: c=3.0		case 12: c=5.0	
	α_{opt}	ξ_m	α_{opt}	ξ_m	α_{opt}	ξ_m	α_{opt}	ξ_m	α_{opt}	ξ_m	α_{opt}	ξ_m
1	0	5,5%	0	5,8%	0	5,2%	0		0	7,0%	0	5,8%
2	1	5,6%	1	3,6%	1	3,2%	1		1	4,3%	1	3,6%
3	0	2,8%	0	0,1%	0	0,1%	0		0	0,1%	0	0,1%
4	0	15,3%	0	9,4%	0	8,4%	0		0	11,1%	0	9,2%
5	1	20,5%	1	25,6%	1	23,1%	1		1	30,7%	0	25,5%
6	0	11,7%	0	8,7%	0	7,9%	0		0	10,5%	0	8,7%
7	0	0,0%	0	0,0%	0	0,0%	0		0	0,0%	0	0,0%
8	1	0,0%	1	0,0%	1	0,0%	1		0	0,0%	0	0,0%
9	0	0,0%	0	0,0%	0	0,0%	0		0	0,0%	0	0,0%
10	1	0,0%	0	0,0%	0	0,0%	0		0	0,0%	0	0,0%
11	0	0,0%	0	0,0%	0	0,0%	0		0	0,0%	0	0,0%
12	0	0,1%	0	0,1%	0	0,1%	0		0	0,2%	0	0,2%
13	0		0		0		0		0		0	
14	1		1		0		0		0		0	
15	0		0		0		0		0		0	
16	0		0		0		0		0		0	

$$\diamond \xi_{|target} = 10\%$$

location/ mode	case 1: c=0.8		case 2: c=0.9		case 3: c=1		case 4: c=1.5		case 5: c=2		case 6: c=5		case 7: c=10	
	$\alpha_{ opt}$	ξ_m	$\alpha_{ e}$	ξ_m	$\alpha_{ op}$	ξ_m	$\alpha_{ opt}$	ξ_m	$\alpha_{ opt}$	ξ_m	$\alpha_{ opt}$	ξ_m	$\alpha_{ e}$	ξ_m
1	1	10,5%	0	10,5%	0	10,2%	0	0	11,0%	0	0	11,6%		
2	1	16,0%	1	16,2%	1	15,9%	1	1	11,1%	1	1	7,2%		
3	1	25,5%	1	25,3%	1	24,3%	0	0	5,5%	0	0	0,2%		
4	1	30,7%	1	31,2%	0	30,9%	0	0	30,6%	0	0	18,4%		
5	1	34,0%	1	36,1%	1	37,6%	1	1	40,9%	1	0	51,0%		
6	1	31,3%	1	34,7%	1	38,0%	0	0	23,3%	0	0	17,5%		
7	1	0,0%	1	0,0%	0	0,0%	0	0	0,0%	0	0	0,0%		
8	1	0,0%	1	0,0%	1	0,0%	1	1	0,0%	0	0	0,0%		
9	1	0,0%	1	0,0%	1	0,0%	0	0	0,0%	0	0	0,0%		
10	1	0,0%	1	0,0%	1	0,0%	1	1	0,0%	0	0	0,0%		
11	1	0,0%	1	0,0%	1	0,0%	0	0	0,0%	0	0	0,0%		
12	0	3,1%	0	2,2%	0	2,0%	0	0	0,2%	0	0	0,4%		
13	1		0		0		0	0		0	0			
14	1		1		1		1	1		0	0			
15	1		1		1		1	0		0	0			
16	1		1		1		1	0		0	0			

$$\diamond \xi_{|target} = 15\%$$

location/ mode	case 1: c=1.2		case 2: c=1.5		case 3: c=2		case 4: c=5		case 5: c=10		case 6: c=15	
	$\alpha_{ opt}$	ξ_m	$\alpha_{ opt}$	ξ_m	$\alpha_{ opt}$	ξ_m	$\alpha_{ opt}$	ξ_m	$\alpha_{ opt}$	ξ_m	$\alpha_{ opt}$	ξ_m
1	1	15,8%	0	19,7%	0		0	0	23,3%	0		
2	1	24,0%	1	30,0%	1		1	1	14,4%	1		
3	1	38,3%	1	47,9%	0		0	0	0,4%	0		
4	1	46,1%	0	57,6%	0		0	0	37,1%	0		
5	1	51,0%	1	63,7%	1		1	1	102,4%	0		
6	1	47,0%	1	58,8%	0		0	0	35,0%	0		
7	1	0,0%	0	0,0%	0		0	0	0,0%	0		
8	1	0,0%	1	0,0%	1		1	0	0,0%	0		
9	1	0,0%	1	0,0%	1		0	0	0,0%	0		
10	1	0,0%	1	0,0%	1		0	0	0,0%	0		
11	1	0,0%	1	0,0%	0		0	0	0,0%	0		
12	0	4,6%	0	5,8%	0		0	0	0,5%	0		
13	1		0		0		0	0		0		
14	1		1		1		0	0		0		
15	1		1		1		0	0		0		
16	1		1		1		0	0		0		

$$\diamond \xi_{|target} = 20\%$$

location/ mode	case 1: c=1.5		case 2: c=2		case 3: c=5		case 4: c=10		case 5: c=20	
	α_{opt}	ξ_m	α_{opt}	ξ_m	α_{opt}	ξ_m	α_{opt}	ξ_m	α_{opt}	ξ_m
1	1	20,2%	0	20,4%	0	23,2%	0	23,3%	0	23,3%
2	1	36,1%	1	31,8%	1	14,5%	1	14,4%	1	14,4%
3	1	59,9%	1	48,6%	0	0,3%	0	0,4%	0	0,4%
4	1	71,0%	0	61,8%	0	37,4%	0	37,1%	0	36,9%
5	1	78,2%	1	75,2%	1	102,3%	1	102,4%	0	101,9%
6	1	74,3%	1	76,0%	0	34,7%	0	35,0%	0	34,9%
7	1	0,0%	0	0,0%	0	0,0%	0	0,0%	0	0,0%
8	1	0,1%	1	0,0%	1	0,0%	0	0,0%	0	0,0%
9	1	0,0%	1	0,0%	0	0,0%	0	0,0%	0	0,0%
10	1	0,0%	1	0,0%	0	0,0%	0	0,0%	0	0,0%
11	1	0,0%	1	0,1%	0	0,0%	0	0,0%	0	0,0%
12	1	5,8%	0	4,0%	0	0,5%	0	0,5%	0	0,8%
13	1		0		0		0		0	
14	1		1		1		0		0	
15	1		1		0		0		0	
16	1		1		0		0		0	

$$\diamond \xi_{|target} = 25\%$$

location/ mode	case 1: c=1.9		case 2: c=2.5		case 3: c=5		case 4: c=10		case 5: c=20	
	α_{opt}	ξ_m	α_{opt}	ξ_m	α_{opt}	ξ_m	α_{opt}	ξ_m	α_{opt}	ξ_m
1	1	25,0%	0	25,6%	0	27,4%	0	34,8%	0	46,5%
2	1	38,0%	1	39,8%	1	27,8%	1	21,7%	1	28,8%
3	1	60,6%	1	60,8%	0	13,8%	0	0,5%	0	0,7%
4	1	72,9%	0	77,2%	0	76,5%	0	56,0%	0	74,2%
5	1	80,7%	1	94,0%	1	102,3%	1	153,7%	1	204,7%
6	1	74,5%	1	94,9%	0	58,3%	0	52,4%	0	70,0%
7	1	0,0%	0	0,0%	0	0,0%	0	0,0%	0	0,0%
8	1	0,0%	1	0,0%	1	0,0%	1	0,0%	0	0,0%
9	1	0,0%	1	0,0%	0	0,0%	0	0,0%	0	0,0%
10	1	0,0%	1	0,0%	1	0,0%	0	0,0%	0	0,0%
11	1	0,1%	1	0,1%	0	0,0%	0	0,0%	0	0,0%
12	0	7,3%	0	5,0%	0	0,6%	0	0,6%	0	1,0%
13	1		0		0		0		0	
14	1		1		1		0		0	
15	1		1		0		0		0	
16	1		1		0		0		0	

$$\diamond \xi_{1|t \text{ arg et}} = 30\%$$

location/mode	case 1: c=2.3		case 2: c=2.5		case 3: c=5		case 4: c=10		case 5: c=20	
	α_{opt}	ξ_m	α_{opt}	ξ_m	α_{opt}	ξ_m	α_{opt}	ξ_m	α_{opt}	ξ_m
1	1	30,3%	0		0	31,6%	0	34,8%	0	46,5%
2	1	46,1%	1		1	40,7%	1	21,7%	1	28,8%
3	1	73,4%	1		0	27,3%	0	0,5%	0	0,7%
4	1	88,3%	1		0	115,1%	0	56,0%	0	74,2%
5	1	97,7%	1		1	102,3%	1	153,7%	1	204,7%
6	1	90,1%	1		0	82,1%	0	52,4%	0	70,0%
7	1	0,0%	1		0	0,0%	0	0,0%	0	0,0%
8	1	0,0%	1		1	0,0%	1	0,0%	0	0,0%
9	1	0,0%	1		0	0,0%	0	0,0%	0	0,0%
10	1	0,0%	1		1	0,0%	0	0,0%	0	0,0%
11	1	0,1%	1		0	0,0%	0	0,0%	0	0,0%
12	0	8,9%	0		0	0,7%	0	0,6%	0	1,0%
13	1		1		0		0		0	
14	1		1		1		0		0	
15	1		1		0		0		0	
16	1		1		1		0		0	

Case study 2: $\xi_{m|t \text{ arg et}}$ has two non-zero values, $\xi_{1|t \text{ arg et}} > \xi_{2|t \text{ arg et}}$

$$\diamond \xi_{1|t \text{ arg et}} = 0\%, \xi_{2|t \text{ arg et}} = 10\%$$

location/mode	case 1: c=0.5		case 2: c=0.8		case 3: c=1		case 4: c=1.5	
	α_{opt}	ξ_m	α_{opt}	ξ_m	α_{opt}	ξ_m	α_{opt}	ξ_m
1	1	2,5%	0	1,5%	0	1,2%	0	1,2%
2	0	10,1%	0	11,6%	0	11,8%	0	11,6%
3	0	11,6%	0	11,8%	0	12,1%	0	6,1%
4	1	15,1%	0	13,4%	0	8,9%	0	0,0%
5	0	9,6%	0	12,4%	0	15,5%	0	8,7%
6	0	16,1%	0	21,2%	0	21,8%	0	17,2%
7	1	0,0%	0	0,0%	0	0,0%	0	0,0%
8	0	0,0%	0	0,1%	0	0,1%	0	0,0%
9	0	0,0%	0	0,0%	0	0,0%	0	0,0%
10	1	0,0%	1	0,0%	0	0,0%	0	0,0%
11	1	0,0%	1	0,0%	1	0,0%	1	0,0%
12	1	0,6%	1	0,0%	1	0,0%	0	0,0%
13	0		0		0		0	
14	0		0		0		0	
15	0		0		0		0	
16	1		0		0		0	

$$\diamond \zeta_{1|target} = 0\%, \zeta_{2|target} = 20\%$$

location/mode	case 1: c=1	
	α_{opt}	ξ_m
1	1	4,9%
2	0	20,1%
3	0	23,2%
4	1	30,1%
5	0	19,1%
6	0	32,2%
7	1	0,0%
8	0	0,1%
9	0	0,0%
10	1	0,0%
11	1	0,0%
12	1	1,2%
13	0	
14	0	
15	0	
16	1	

$$\diamond \zeta_{1|target} = 20\%, \zeta_{2|target} = 20\%$$

location/mode	case 1: c=5		case 2: c=3		case 3: c=6		case 4: c=10		case 5: c=20	
	α_{opt}	ξ_m	α_{opt}	ξ_m	α_{opt}	ξ_m	α_{opt}	ξ_m	α_{opt}	ξ_m
1	0	27,1%	0	21,4%	0	25,6%	0	31,0%	0	38,9%
2	1	53,1%	1	24,5%	1	59,4%	1	91,7%	1	169,0%
3	0	20,6%	0	27,7%	0	24,6%	0	40,8%	0	81,2%
4	0	37,5%	0	74,6%	0	33,7%	0	37,3%	0	37,2%
5	1	131,4%	1	69,8%	1	127,1%	1	160,6%	0	218,3%
6	0	92,2%	0	56,5%	0	100,4%	0	149,9%	0	264,8%
7	0	0,0%	0	0,0%	0	0,0%	0	0,0%	0	0,0%
8	1	0,0%	1	0,0%	1	0,0%	0	0,0%	0	0,1%
9	0	0,0%	0	0,0%	0	0,0%	0	0,0%	0	0,0%
10	0	0,0%	1	0,0%	0	0,0%	0	0,0%	0	0,0%
11	1	0,0%	0	0,0%	1	0,0%	1	0,0%	1	0,0%
12	0	0,5%	0	2,6%	0	0,4%	0	0,5%	0	0,8%
13	0		0		0		0		0	
14	1		1		0		0		0	
15	0		1		0		0		0	
16	0		1		0		0		0	

Case study 3: $\xi_{m|t \text{ arg et}}$ has three non-zero values, $\xi_{1|t \text{ arg et}}, \xi_{2|t \text{ arg et}}, \xi_{3|t \text{ arg et}}$

❖ $\xi_{1|t \text{ arg et}} = \xi_{2|t \text{ arg et}} = 0\%, \xi_{3|t \text{ arg et}} = 10\%$

location/mode	case 1: c=0.5		case 2: c=0.8		case 3: c=1		case 4: c=1.3	
	α_{opt}	ξ_m	α_{opt}	ξ_m	α_{opt}	ξ_m	α_{opt}	ξ_m
1	0	1,7%	0	1,5%	0	1,1%	0	0,4%
2	0	5,9%	0	9,4%	0	11,8%	0	5,3%
3	0	11,6%	0	12,7%	0	12,1%	0	10,4%
4	0	7,4%	0	8,6%	0	8,9%	0	11,6%
5	0	12,0%	0	14,6%	0	15,5%	0	12,6%
6	1	14,6%	0	19,4%	0	21,8%	0	13,4%
7	0	0,0%	0	0,0%	0	0,0%	0	0,0%
8	0	0,0%	0	0,1%	0	0,1%	0	0,1%
9	1	0,0%	0	0,0%	0	0,0%	0	0,0%
10	0	0,0%	0	0,0%	0	0,0%	0	0,0%
11	1	0,0%	1	0,0%	1	0,0%	0	0,0%
12	1	0,6%	1	0,6%	1	0,0%	1	0,0%
13	0		0		0		0	
14	0		0		0		0	
15	1		1		0		0	
16	0		0		0		0	

❖ $\xi_{1|t \text{ arg et}} = \xi_{2|t \text{ arg et}} = 0\%, \xi_{3|t \text{ arg et}} = 20\%$

location/mode	case 1: c=1	
	α_{opt}	ξ_m
1	0	3,3%
2	0	9,5%
3	1	21,5%
4	0	13,4%
5	0	21,5%
6	1	25,5%
7	0	0,0%
8	0	0,1%
9	1	0,0%
10	0	0,0%
11	1	0,0%
12	1	1,5%
13	0	
14	0	
15	1	
16	0	

$$\diamond \xi_{1|t \text{ arg et}} = \xi_{2|t \text{ arg et}} = \xi_{3|t \text{ arg et}} = 20\%$$

location/mode	case 1: c=1.5		case 2: c=3		case 3: c=5		case 4: c=8		case 5: c=15		case 6: c=100,000	
	α_{opt}	ξ_m	α_{opt}	ξ_m	α_{opt}	ξ_m	α_{opt}	ξ_m	α_{opt}	ξ_m	α_{opt}	ξ_m
1	1	20,2%	0	21,4%	0	21,3%	0	0	0	29,1%	0	0
2	1	36,1%	1	24,5%	1	49,5%	1	1	1	126,8%	1	1
3	1	59,9%	0	27,7%	0	20,5%	0	0	0	60,9%	0	0
4	1	71,0%	0	74,6%	0	28,1%	0	0	0	27,9%	0	0
5	1	78,2%	1	69,8%	1	106,0%	1	0	0	163,7%	0	0
6	1	74,3%	0	56,5%	0	83,7%	0	0	0	198,6%	0	0
7	1	0,0%	0	0,0%	0	0,0%	0	0	0	0,0%	0	0
8	1	0,1%	1	0,0%	1	0,0%	0	0	0	0,0%	0	0
9	1	0,0%	0	0,0%	0	0,0%	0	0	0	0,0%	0	0
10	1	0,0%	1	0,0%	0	0,0%	0	0	0	0,0%	0	0
11	1	0,0%	0	0,0%	1	0,0%	1	1	1	0,0%	1	1
12	1	5,8%	0	2,6%	0	0,3%	0	0	0	0,6%	0	0
13	1		0		0		0	0	0		0	0
14	1		1		0		0	0	0		0	0
15	1		1		0		0	0	0		0	0
16	1		1		0		0	0	0		0	0

$$\diamond \xi_{1|t \text{ arg et}} = \xi_{2|t \text{ arg et}} = \xi_{3|t \text{ arg et}} = 30\%$$

location/mode	case 1: c=3		case 2: c=5		case 3: c=10	
	α_{opt}	ξ_m	α_{opt}	ξ_m	α_{opt}	ξ_m
1	0	30,7%	0		0	
2	1	47,8%	1		1	
3	1	72,9%	0		0	
4	0	92,6%	0		0	
5	1	112,9%	1		1	
6	1	113,9%	0		0	
7	0	0,0%	0		0	
8	1	0,0%	1		1	
9	1	0,0%	0		0	
10	1	0,0%	1		0	
11	1	0,1%	1		1	
12	0	6,0%	0		0	
13	0		0		0	
14	1		1		0	
15	1		1		0	
16	1		0		0	

Case study 4: $\xi_{m|t \text{ arg et}}$ has four non-zero values, $\xi_{1|t \text{ arg et}}, \xi_{2|t \text{ arg et}}, \xi_{3|t \text{ arg et}}, \xi_{4|t \text{ arg et}}$

❖ $\xi_{1|t \text{ arg et}} = \xi_{2|t \text{ arg et}} = \xi_{3|t \text{ arg et}} = 0\%, \xi_{4|t \text{ arg et}} = 10\%$

location/mode	case 1: c=0.3		case 2: c=0.5		case 3: c=1		case 4: c=5	
	α_{opt}	ξ_m	α_{opt}	ξ_m	α_{opt}	ξ_m	α_{opt}	ξ_m
1	0	2,0%	0	1,0%	0	1,1%	0	1,4%
2	0	3,2%	0	4,7%	0	6,7%	0	20,3%
3	1	7,3%	0	6,7%	0	10,7%	0	40,1%
4	0	10,3%	0	12,2%	0	16,7%	0	44,6%
5	0	8,5%	0	4,8%	0	9,7%	0	48,3%
6	1	9,3%	0	9,9%	0	15,0%	0	51,6%
7	0	0,0%	0	0,0%	0	0,0%	0	0,1%
8	1	0,0%	0	0,0%	0	0,1%	0	0,3%
9	1	0,0%	0	0,0%	0	0,0%	0	0,0%
10	1	0,0%	1	0,0%	1	0,0%	0	0,0%
11	0	0,0%	0	0,0%	0	0,0%	0	0,0%
12	1	0,4%	1	0,0%	1	0,0%	1	0,0%
13	0		0		0		0	
14	1		0		0		0	
15	0		0		0		0	
16	1		1		0		0	

❖ $\xi_{1|t \text{ arg et}} = \xi_{2|t \text{ arg et}} = \xi_{3|t \text{ arg et}} = 0\%, \xi_{4|t \text{ arg et}} = 20\%$

location/mode	case 1: c=0.5		case 2: c=1		case 3: c=5	
	α_{opt}	ξ_m	α_{opt}	ξ_m	α_{opt}	ξ_m
1	1	4,8%	0	2,0%	0	1,4%
2	0	7,4%	0	9,3%	0	20,3%
3	1	16,0%	0	13,4%	0	40,1%
4	1	20,9%	0	24,5%	0	44,6%
5	0	16,6%	0	9,7%	0	48,3%
6	1	16,1%	0	19,8%	0	51,6%
7	1	0,0%	0	0,0%	0	0,1%
8	1	0,0%	0	0,1%	0	0,3%
9	1	0,0%	0	0,0%	0	0,0%
10	1	0,0%	1	0,0%	0	0,0%
11	0	0,0%	0	0,0%	0	0,0%
12	1	1,5%	1	0,0%	1	0,0%
13	1		0		0	
14	1		0		0	
15	0		0		0	
16	1		1		0	

$$\diamond \xi_{1|target} = \xi_{2|target} = \xi_{3|target} = \xi_{4|target} = 20\%$$

location/mode	case 1: c=1.5		case 2: c=2		case 3: c=5	
	α_{opt}	ξ_m	α_{opt}	ξ_m	α_{opt}	ξ_m
1	1	20,2%	0	20,4%	0	0
2	1	36,1%	1	31,8%	1	0
3	1	59,9%	1	48,6%	0	0
4	1	71,0%	0	61,8%	0	0
5	1	78,2%	1	75,2%	1	0
6	1	74,3%	1	76,0%	0	0
7	1	0,0%	0	0,0%	0	0
8	1	0,1%	1	0,0%	1	0
9	1	0,0%	1	0,0%	0	0
10	1	0,0%	1	0,0%	0	0
11	1	0,0%	1	0,1%	1	0
12	1	5,8%	0	4,0%	0	0
13	1		0		0	0
14	1		1		0	0
15	1		1		0	0
16	1		1		0	0

$$\diamond \xi_{1|target} = \xi_{2|target} = \xi_{3|target} = \xi_{4|target} = 30\%$$

location/mode	case 1: c=3		case 2: c=5		case 3: c=7		case 4: c=10	
	α_{opt}	ξ_m	α_{opt}	ξ_m	α_{opt}	ξ_m	α_{opt}	ξ_m
1	0	30,7%	0		0		0	
2	1	47,8%	1		1		1	
3	1	72,9%	0		0		0	
4	0	92,6%	0		0		0	
5	1	112,9%	1		1		1	
6	1	113,9%	0		0		0	
7	0	0,0%	0		0		0	
8	1	0,0%	1		1		1	
9	1	0,0%	0		0		0	
10	1	0,0%	1		0		0	
11	1	0,1%	1		1		1	
12	0	6,0%	0		0		0	
13	0		0		0		0	
14	1		1		0		0	
15	1		1		1		0	
16	1		0		0		0	

Case study 5: $\xi_{m|t \text{ arg et}}$ has five non-zero values, $\xi_{1|t \text{ arg et}}, \xi_{2|t \text{ arg et}}, \xi_{3|t \text{ arg et}}, \xi_{4|t \text{ arg et}}, \xi_{5|t \text{ arg et}}$

❖ $\xi_{1|t \text{ arg et}} = \xi_{2|t \text{ arg et}} = \xi_{3|t \text{ arg et}} = \xi_{4|t \text{ arg et}} = 0\%, \xi_{5|t \text{ arg et}} = 10\%$

location/mode	case 1: c=0.2		case 2: c=0.5		case 3: c=1		case 4: c=5	
	α_{opt}	ξ_m	α_{opt}	ξ_m	α_{opt}	ξ_m	α_{opt}	ξ_m
1	1	2,2%	0	1,1%	0		0	1,4%
2	1	3,6%	0	6,3%	0		0	20,3%
3	1	6,5%	0	6,0%	0		0	40,1%
4	1	6,0%	0	5,4%	0		0	44,6%
5	1	10,2%	1	10,3%	0		0	48,3%
6	1	7,9%	0	11,8%	0		0	51,6%
7	1	0,0%	0	0,0%	0		0	0,1%
8	1	0,0%	0	0,0%	0		0	0,3%
9	1	0,0%	0	0,0%	0		0	0,0%
10	0	0,0%	0	0,0%	0		0	0,0%
11	1	0,0%	1	0,0%	1		0	0,0%
12	1	0,6%	1	0,0%	1		1	0,0%
13	0		0		0		0	
14	1		0		0		0	
15	1		0		0		0	
16	0		0		0		0	

❖ $\xi_{1|t \text{ arg et}} = \xi_{2|t \text{ arg et}} = \xi_{3|t \text{ arg et}} = \xi_{4|t \text{ arg et}} = 0\%, \xi_{5|t \text{ arg et}} = 20\%$

location/mode	case 1: c=0.5		case 2: c=1		case 3: c=5	
	α_{opt}	ξ_m	α_{opt}	ξ_m	α_{opt}	ξ_m
1	0		0	2,2%	0	1,4%
2	1		0	12,5%	0	20,3%
3	0		0	12,1%	0	40,1%
4	0		0	10,8%	0	44,6%
5	1		1	20,6%	0	48,3%
6	1		0	23,6%	0	51,6%
7	0		0	0,0%	0	0,1%
8	1		0	0,1%	0	0,3%
9	1		0	0,0%	0	0,0%
10	0		0	0,0%	0	0,0%
11	1		1	0,0%	0	0,0%
12	1		1	0,0%	1	0,0%
13	0		0		0	
14	1		0		0	
15	0		0		0	
16	0		0		0	

$$\diamond \xi_{1|target} = \xi_{2|target} = \xi_{3|target} = \xi_{4|target} = \xi_{5|target} = 20\%$$

location/mode	case 1: c=1.5		case 2: c=2	
	α_{opt}	ξ_m	α_{opt}	ξ_m
1	1	20,2%	0	20,4%
2	1	36,1%	1	31,8%
3	1	59,9%	1	48,6%
4	1	71,0%	0	61,8%
5	1	78,2%	1	75,2%
6	1	74,3%	1	76,0%
7	1	0,0%	0	0,0%
8	1	0,1%	1	0,0%
9	1	0,0%	1	0,0%
10	1	0,0%	1	0,0%
11	1	0,0%	1	0,1%
12	1	5,8%	0	4,0%
13	1		0	
14	1		1	
15	1		1	
16	1		1	

$$\diamond \xi_{1|target} = \xi_{2|target} = \xi_{3|target} = \xi_{4|target} = \xi_{5|target} = 30\%$$

location/mode	case 1: c=5		case 2: c=10		case 3: c=15	
	α_{opt}	ξ_m	α_{opt}	ξ_m	α_{opt}	ξ_m
1	0	35,3%	0	35,3%	0	46,6%
2	1	66,5%	1	66,5%	1	137,6%
3	0	52,9%	0	52,9%	0	61,2%
4	0	85,8%	0	85,8%	0	55,9%
5	1	145,4%	1	145,4%	1	240,8%
6	0	127,8%	0	127,8%	0	224,9%
7	0	0,0%	0	0,0%	0	0,0%
8	1	0,0%	1	0,0%	0	0,0%
9	0	0,0%	0	0,0%	0	0,0%
10	1	0,0%	0	0,0%	0	0,0%
11	1	0,1%	1	0,1%	1	0,0%
12	0	4,2%	0	4,2%	0	0,8%
13	0		0		0	
14	1		0		0	
15	1		0		0	
16	0		0		0	

Case study 6: $\xi_{m|t \text{ arg et}}$ has six non-zero values, $\xi_{1|tar}, \xi_{2|tar}, \xi_{3|tar}, \xi_{4|tar}, \xi_{5|tar}, \xi_{6|tar}$

❖ $\xi_{1|t \text{ arg et}} = \xi_{2|t \text{ arg et}} = \xi_{3|t \text{ arg et}} = \xi_{4|t \text{ arg et}} = \xi_{5|t \text{ arg et}} = 0\%, \xi_{6|t \text{ arg et}} = 10\%$

location/mode	case 1: c=0.3		case 2: c=0.5	
	α_{opt}	ξ_m	α_{opt}	ξ_m
1	0		0	
2	0		0	
3	1		0	
4	0		0	
5	0		0	
6	0		0	
7	0		0	
8	0		0	
9	0		0	
10	1		0	
11	1		1	
12	1		1	
13	0		0	
14	0		0	
15	0		0	
16	1		0	

❖ $\xi_{1|t \text{ arg et}} = \xi_{2|t \text{ arg et}} = \xi_{3|t \text{ arg et}} = \xi_{4|t \text{ arg et}} = \xi_{5|t \text{ arg et}} = 0\%, \xi_{6|t \text{ arg et}} = 20\%$

location/mode	case 1: c=0.5		case 2: c=1	
	α_{opt}	ξ_m	α_{opt}	ξ_m
1	0	2,9%	0	
2	0	8,5%	0	
3	1	16,1%	0	
4	0	16,2%	0	
5	0	13,4%	0	
6	1	20,7%	0	
7	0	0,0%	0	
8	0	0,0%	0	
9	1	0,0%	0	
10	1	0,0%	0	
11	1	0,0%	1	
12	1	1,0%	1	
13	0		0	
14	0		0	
15	0		0	
16	1		0	

$$\diamond \xi_{1|t \text{ arg et}} = \xi_{2|t \text{ arg et}} = \xi_{3|t \text{ arg et}} = \xi_{4|t \text{ arg et}} = \xi_{5|t \text{ arg et}} = \xi_{6|t \text{ arg et}} = 20\%$$

location/mode	case 1: c=1.5		case 2: c=2	
	$\alpha_{ opt}$	ξ_m	$\alpha_{ opt}$	ξ_m
1	1	20,2%	0	20,4%
2	1	36,1%	1	31,8%
3	1	59,9%	1	48,6%
4	1	71,0%	0	61,8%
5	1	78,2%	1	75,2%
6	1	74,3%	1	76,0%
7	1	0,0%	0	0,0%
8	1	0,1%	1	0,0%
9	1	0,0%	1	0,0%
10	1	0,0%	1	0,0%
11	1	0,0%	1	0,1%
12	1	5,8%	0	4,0%
13	1		0	
14	1		1	
15	1		1	
16	1		1	

Case study 7: mode 12 for $\xi_{12|t \text{ arg et}} = 10\%$

location/mode	case 1: c=3		case 2: c=5	
	$\alpha_{ opt}$	ξ_m	$\alpha_{ opt}$	ξ_m
1	1	15,8%	1	
2	0	12,4%	0	
3	1	56,2%	0	
4	1	40,1%	0	
5	0	40,1%	0	
6	0	26,1%	0	
7	1	0,0%	0	
8	0	0,0%	0	
9	1	0,0%	0	
10	0	0,0%	0	
11	0	0,1%	0	
12	0	10,5%	0	
13	1		1	
14	0		0	
15	1		1	
16	0		0	